Cingulate retinoic acid signaling regulates neuropathic pain and comorbid anxiodepression via extracellular matrix homeostasis

Zhen-Zhen Li[1, 2#], Wan-Neng Liu[1#], Ke-Xin Liu[1#], Zhi-Wei Dou[1], Rui Zhao[3], Yun Chen[1], Meng-Meng Wang[1], Tao-Zhi Wang[4], Fei Wang[1], Wen-Juan Han[1], Wen-Guang Chu[1], Xing-Xing Zheng[1], Rou-Gang Xie[1], Hua Yuan[3], Xiao-Fan Jiang[2], Xiao-Long Sun[3*], Ceng Luo[1*], Sheng-Xi Wu[1*]

[1] Department of Neurobiology, School of Basic Medicine, [2] Department of Neurosurgery, Xijing Hospital, [3] Department of Rehabilitation Medicine, Xijing Hospital, and [4] Department of Anesthesiology and Perioperative Medicine, Xijing Hospital, Fourth Military Medical University, Xi'an 710032, China.

[#]These authors contributed to this work equally.

*Correspondence should be addressed to Sheng-Xi Wu at shengxi@fmmu.edu.cn or Ceng Luo at luoceng@fmmu.edu.cn or Xiao-Long Sun at xlsun@fmmu.edu.cn.

Phone: (86)-29-84712312

Abstract

Neuropathic pain is often comorbid with affective disorders. Synaptic plasticity in anterior cingulate cortex (ACC) is assumed to be a crucial interface for pain perception and emotion. Laminin β1 (LAMB1), a key element of extracellular matrix (ECM) in ACC was recently revealed to convey extracellular alterations to intracellular synaptic plasticity and underlie neuropathic pain and aversive emotion. However, it remains elusive what triggers activity-dependent changes of LAMB1 and ECM remodeling after nerve injury. Here, we uncovered a key role of retinoic acid (RA)/RARB signaling in neuropathic pain and associated anxiodepression via regulation of ECM homeostasis. We showed that nerve injury reduced RA level in the serum and ACC in mice and human, which brought about downregulation of its corresponding receptor, RARB. Overexpressing RARB relieved pain hypersensitivity and comorbid anxiodepression, while silencing RARB exacerbated pain sensitivity and induced anxiodepression. Further mechanistic analysis revealed that RARB maintained ECM homeostasis via transcriptional regulation of LAMB1, reversing abnormal synaptic plasticity and eventually improved neuropathic pain and aversive emotion. Taken together with our previous study, we revealed an intracellular-extracellular-intracellular feedforward regulatory network in modulating pain plasticity. Moreover, we identified cingulate RA/RARB signaling as a promising therapeutic target for treatment of neuropathic pain and associated anxiodepression.

Introduction

Chronic neuropathic pain frequently leads to emotional disturbances, such as anxiety and depression, which in turn exacerbates the severity and prolongs the duration of pain. This results in a vicious cycle between pain and anxiodepression, rendering neuropathic pain more intractable and resistant to traditional analgesics (1). Thus, exploiting a new and effective treatment for the comorbidity of neuropathic pain and affective disorders remains a major challenge (1).

Mounting evidence has documented the key significance of anterior cingulate cortex (ACC) as a critical interface for pain perception and emotional response (2-4). Following nerve injury, ACC neurons get activated, and inhibition of cingulate plasticity produces analgesic, anxiolytic and antidepressive effects (5-9). Despite these advances, much attention thus far has been paid on intracellular mechanisms of cingulate plasticity rather than extracellular alterations that might trigger and promote intracellular changes (10). Interestingly, we recently demonstrated an activity-dependent remodeling of extracellular matrix (ECM) in the ACC after nerve injury and revealed a new mechanism by which a key element of ECM, laminin β1 (LAMB1), conveys extracellular alterations to intracellular structural and functional plasticity and thus underlies neuropathic pain and anxiodepressive consequences (11). However, it remains elusive what triggers activity-dependent changes of LAMB1 and further ECM remodeling after nerve injury. Which signaling

cascades are involved in this process?

It has shown that LAMB1 is mainly expressed in neurons and then secreted into extracellular space in the ACC (11). This suggests that an upstream intracellular cascade might be involved in triggering activity-dependent changes of ECM LAMB1 after nerve injury. In several murine and human cell lines, a retinoic acid response element (RARE) has been identified within the 5′-flanking region of *Lamb1* gene (12). As a nuclear receptor superfamily, retinoic acid receptors (RARs), consisting of α, β and γ subunits (13), function as transcription factors by binding to the RARE in the promoters of target genes, which is involved in neuronal development and synaptic plasticity homeostasis, ultimately affecting multiple brain functions (13-16). For example, amongst RARs subtypes, RARB shows preferential binding to the RARE of *Lamb1* promoter and trigger *Lamb1* transcription in murine cell lines (17). In adult mouse brain, RARB possesses the ability to modulate social cognition and spatial memory by regulating long-term potentiation (LTP) in the hippocampus (18, 19). However, very little is known about whether and how RARB regulates transcription of LAMB1 in the ACC and thus contributes to neuropathic pain and comorbid anxiodepression.

It is well known that the expression level and activity of RARB are regulated by its ligand retinoic acid (RA) (13, 14, 20) . RA metabolic disturbance has been linked with affective disorders in clinical trials (21-23). As a metabolic product of retinol (vitamin A), the synthesis and metabolism of RA are strictly regulated

in temporal and spatial dimension, thus controlling rational distribution of RA (24-26). RALDH (retinaldehyde dehydrogenases) acts to catalyze the retinol into biologically active RA, while CYP26 (cytochrome P450 family 26), as a metabolic enzyme, leads to the oxidization of RA (27, 28). Early studies of vitamin A and RA have been mainly focusing on the eye, skin, immune and reproductive systems (28, 29). Nevertheless, emerging evidence has shown that controlled RA synthesis is essential for regulating homeostatic synaptic plasticity (30, 31). RA deficiency is closely associated with a variety of brain diseases, i.e. developmental impairment, affective disorders, cognitive dysfunction (21, 23, 32, 33). However, it remains elusive whether RA metabolic homeostasis is disturbed during pain chronicity? If so, would it affect ECM remodeling via regulation of RARB in the ACC and ultimately exacerbates pain responses and related negative emotion?

By using multiple cutting-edge approaches, we uncovered a key role of cingulate RA/RARB signaling in neuropathic pain and associated anxiodepression via regulation of ECM homeostasis. Following nerve injury, RA is significantly reduced in the serum and ACC of mice and human. This brings about the downregulation of its corresponding receptor, RARB. Overexpression of RARB relieves pain hypersensitivity and comorbid anxiodepression, while knockdown of RARB exacerbates pain sensitivity and induces anxiodepression. Further mechanistic analysis revealed that RARB acts to maintain ECM homeostasis via regulation of LAMB1 transcription, leading to stabilize the

abnormal structural and functional plasticity of pyramidal neurons and eventually produces analgesic, anxiolytic and antidepressive effects. We believe this study sheds new light on the functional capability of RA/RARB homeostasis in modulating neuropathic pain and associated anxiodepression via interaction with ECM LAMB1. Taken together with our previous study (11), we revealed an intracellular-extracellular-intracellular feedforward regulatory network underlying the comorbidity of neuropathic pain and anxiodepression. Moreover, we have identified cingulate RA/RARB signaling as a promising therapeutic target for treatment of neuropathic pain and associated anxiodepression.

Results

RARB as a transcriptional factor is decreased in the ACC after peripheral neuropathy

As we described previously (11), following a long-lasting pain hypersensitivity and comorbid anxiodepression caused by spared nerve injury (SNI), LAMB1, a key element of ECM, was significantly downregulated. To identify the potential transcriptional factors of LAMB1 that are involved in the process of neuropathic pain and associated anxiodepression, we analyzed the differentially expressed genes from RNA-seq data in the ACC on day 56 after SNI. We identified 10 differential changes of transcription factors related with *Lamb1* (Figure 1A). Amongst which, RARB showed stronger relation with *Lamb1* and involved in several physiopathological processes (12). We further verified differences at mRNA and protein levels by quantitative real-time PCR and immunoblotting in contralateral ACC at different time points after SNI, with significant downregulation of RARB on day 56 following SNI (Figure 1, B and C). We then characterized the expression profile of RARB in the ACC. The data revealed that RARB is highly co-expressed with neuronal nuclear antigen (NeuN) and sparsely with either glial fibrillary acidic protein (GFAP) or ionized calcium–binding adapter molecule 1 (Iba1) (Figure 1, D and E). Furthermore, we detected preferential RARB expression in calcium/calmodulin-dependent protein kinase II (CaMKII)-positive neurons (Figure 1, F and G). Together, these data suggest a potential relationship between RARB and neuropathic pain as

well as pain-related anxiodepression.

RARB overexpression in the ACC relieves pain hypersensitivity and anxiodepression caused by nerve injury

To address whether there is a causal relationship between activity-dependent changes of RARB and neuropathic pain and related anxiodepression, we generated a recombinant adeno-associated virions of serotype 2/9 (AAV2/9) expressing mCherry-tagged murine Rarb cDNA (designated as AAV-RARB) under CaMKII promoter. The AAV2/9 expressing mCherry only were served as control (AAV-control). The efficiency of RARB overexpression in the ACC was verified (Figure 2, A-C). We then assessed how overexpression of RARB in contralateral ACC affects pain sensitivity and anxiodepression-like behaviors (Figure 2D). Compared with control mice, overexpressing RARB in the right ACC in SNI-treated mice significantly reduced bilateral mechanical and ipsilateral thermal sensitivity (Figure 2, E-H). In contrast, basal mechanical and thermal nociception in bilateral hindpaws were unaltered by cingulate RARB overexpression (Supplemental Figure 1, A-D).

Neuropathic pain is frequently comorbid with aversive emotions (1). We next observed whether RARB in the ACC relieves neuropathic pain-related anxiety and depression. In the elevated plus maze (EPM) test, SNI-treated mice expressing RARB exhibited frequent traveling in the open arm as compared with control mice (Figure 2I and Supplemental Figure 1E). In the tail suspension

test (TST) and sucrose preference test (SPT), overexpression of cingulate RARB reversed the longer immobility and reduction of sucrose preference in SNI-treated mice (Figure 2, J and K). In sham-treated mice, overexpression of RARB in the ACC did not alter travelling distance in the open arm of EPM paradigm and immobility in TST paradigm as well as sucrose consumption in SPT paradigm (Figure 2, I-K). These behavioral results suggest that RARB supplementation in the ACC relieves pain hypersensitivity and associated anxiodepression induced by peripheral neuropathy.

Overexpression of RARB normalizes the abnormal spine remodeling and potentiated synaptic transmission in ACC pyramidal neurons after nerve injury

Structural and functional synaptic plasticity in the ACC is assumed to be a cellular basis for the comorbidity of chronic pain and anxiodepression (2, 5, 8). Thus, we determined to examine whether supplementing RARB would normalize abnormal structural and functional changes in ACC pyramidal neurons after SNI. First, we examined the dendrite and spine structure of pyramidal neurons via Golgi staining in mice overexpressing RARB and mCherry alone. Sholl analysis revealed that the dendrites complexity of apical and basal dendrites of pyramidal neurons did not show obvious alterations after cingulate RARB overexpression in both sham and SNI conditions (Supplemental Figure 2, A-C). In contrast, overexpression of RARB eliminated

the increase in the densities but not the length of total apical spines after SNI (Figure 3, A and B, Supplemental Figure 2D). Further analysis of spine classification revealed that overexpression of RARB preferentially excluded the increased density of stubby- and mushroom-shaped apical spines after SNI, with little influences on long thin- and filopodia-like apical spines (Figure 3C and Supplemental Figure 2E). Meanwhile, overexpression of RARB exerted similar effect on basal spines (Supplemental Figure 2, F-H). These results indicate that RARB contributes to the stabilization of synaptic spines in cingulate pyramidal neurons.

Next, we examined the functional influences of RARB on the intrinsic excitability and synaptic transmission in ACC pyramidal neurons using whole-cell patch-clamp recording (Figure 3D), which were identified by their morphological and firing properties (34). Passive membrane properties including resting membrane potential (RMP) and membrane resistance (Rm) as well as membrane capacitance (Cm) of ACC pyramidal neurons were comparable between mice expressing RARB and mCherry alone in both sham and SNI conditions (Supplemental Figure 3A). However, the active membrane properties of ACC pyramidal neurons represented significant differences between two genotypes in SNI but not sham condition (Figure 3, D-H). This is characterized by a reduced firing frequency and increased rheobase in pyramidal neurons of SNI-operated mice after overexpression of RARB in the ACC (Figure 3, D-H). The other parameters such as action potential (AP)

threshold, amplitude as well as half-width were unaltered by overexpression of cingulate RARB in both sham and SNI condition (Supplemental Figure 3B).

Furthermore, we observed the depressed synaptic transmission in ACC pyramidal neurons derived from SNI-treated mice after overexpression of RARB. AMPA receptor-mediated evoked excitatory postsynaptic currents (AMPAR-eEPSCs) in pyramidal neurons from layers II/III in the ACC at a holding potential of -70 mV were recorded by applying local stimulation in layers V/VI in the presence of picrotoxin (100 μM), an antagonist of inhibitory synaptic transmission, and AP5 (50 μM), an antagonist of NMDA receptor. The amplitude of AMPAR-eEPSCs was significantly reduced after overexpression of cingulate RARB (Figure 3, I and J). To elucidate whether a presynaptic or postsynaptic mechanism is involved, we first analyzed paired-pulse ratio (PPR), i.e. EPSC2/EPSC1, a well-accepted indication of presynaptic mechanisms (35). Upon overexpression of cingulate RARB, the average amplitude of PPR was significantly increased in SNI-treated ACC pyramidal neurons, indicating a decrease in the transmitter release probability via a presynaptic mechanism (Figure 3, K and L). This was further confirmed by a decrease in miniature EPSCs (mEPSCs) frequency after overexpression of ACC RARB (Figure 3, M and N). In parallel, mEPSCs amplitude was attenuated after supplementing RARB, indicative of a postsynaptic mechanism involved as well (Figure 3, M and N). Overall, these results suggest that supplementation of cingulate RARB alleviates cingulate synaptic potentiation

via both presynaptic and postsynaptic mechanisms.

Overexpression of RARB reverses the exaggerated calcium transients in ACC pyramidal neurons after nerve injury

In further support of the crucial role of RARB on functional changes of ACC pyramidal neurons after nerve injury, we performed fiber photometry recording to monitor the activity of GCaMP6s-expressing pyramidal neurons in response to a wide range of external stimuli applied to cutaneous receptive field as well as during tail suspension (Figure 4A). Overexpression of cingulate RARB significantly relieved the activity of ACC pyramidal neurons, as characterized by a lower calcium transients evoked by peripheral mechanical stimuli, such as von Frey filaments, brush and pinprick as well as radiant heat stimuli in SNI-injured mice expressing RARB than control ones (Figure 4, B-F). Meanwhile, during tail suspension, we observed a reduced calcium transient in ACC pyramidal neurons after overexpression of RARB (Figure 4G). Taken together, we can infer that overexpression of cingulate RARB contributes to normalize the abnormal structural and functional plasticity of pyramidal neurons after peripheral neuropathy.

RARB knockdown in the ACC induces pain hypersensitivity and anxiodepression

To further address whether RARB is necessary and sufficient for neuropathic

pain and related anxiodepression, we generated recombinant AAV2/9 vector expressing an shRNA targeted against RARB and verified its knockdown efficiency (Figure 5, A-C). We first assessed how loss of unilateral cingulate RARB influences nociceptive sensitivity (Figure 5D). As compared to mice expressing scrambled shRNA, mice expressing shRarb in the right ACC showed a greater response to von Frey hairs and thermal stimuli in the bilateral hindpaw under sham condition (Figure 5, E and F, and Supplemental Figure 4, A and B). We then examined whether exogenous knockdown of RARB causes pain-related aversive emotion. In EPM and OFT paradigms, sham-treated mice expressing shRarb traveled shorter distance in the open arm and centre area, as compared to control ones (Figure 5, G and H, and Supplemental Figure 4, C and D). Meanwhile, mice expressing shRarb displayed longer immobility in TST paradigm and less sucrose preference in SPT paradigm in comparison with controls (Figure 5, I and J). Thus, these results further consolidate that cingulate RARB negatively regulates pain sensitivity and related anxiodepression.

We further addressed whether cingulate RARB knockdown-evoked pain hypersensitivity and comorbid anxiodepression is associated with upregulated activity in ACC pyramidal neurons by using *in vivo f*iber photometry recording. In sham condition, GCaMP6s-expressing pyramidal neurons derived from mice expressing shRarb exhibited a higher calcium response in response to a wide range of mechanical stimuli, thermal stimuli as well as tail suspension than

those expressing scramble shRNA (Figure 5, K-N, and Supplemental Figure 4, E-G). These data further confirm that downregulation of RARB in the ACC leads to pain hypersensitivity and comorbid anxiodepression as well as exaggerated cingulate pyramidal neuronal activity.

RARB in the ACC regulates ECM homeostasis via modulation of LAMB1 transcription after nerve injury

RARB functions as a potential transcription factor of LAMB1, a key component of ECM (12). Our recent study shed new light on the key significance of LAMB1 in chronic pain and comorbid anxiodepression (11). We were therefore interested to know whether RARB influences neuropathic pain and related aversive emotion via regulation of LAMB1 expression. First, we examined the changes of LAMB1 level after exogenous intervention of RARB expression in the ACC. Immunoblotting analysis revealed that knockdown or overexpression of cingulate RARB leads to downregulation or upregulation of LAMB1 correspondingly (Figure 6, A and B). Meanwhile, Luciferase assay indicated that overexpression of RARB significantly increased luciferase activity which was modulated by *Lamb1* promoter. A retinoic acid response element (RARE) has been identified within -477 to -432 region of *Lamb1* gene (12). We further constructed the specific mutant *Lamb1* promoter on the luciferase reporter, and observed that luciferase activity was significantly decreased after co-transfection of RARB (Figure 6C). Administration of RA, a ligand of RARB,

elevated luciferase activity after co-transfection of RARB and *Lamb1*-Luc plasmids (Figure 6D). In addition, ChIP assay further confirmed that RARB binds to *Lamb1* promoter, and the binding level was significantly increased after overexpressing RARB (Figure 6E). These data collectively suggest that RARB regulates the expression of LAMB1 as an upstream transcription factor. To further confirm the regulatory relationship between RARB and LAMB1 in neuropathic pain, we infected the ACC with AAV-shLamb1 and overexpressing RARB at an interval of 3 weeks in SNI-treated mice (Figure 6, F and G). We observed that knockdown of LAMB1 excludes the pain relief evoked by overexpression of RARB in SNI-injured mice (Figure 6, H and I). In parallel, RARB-induced anxiolytic effect observed in the OFT paradigm was significantly inhibited in shLamb1-infected mice with SNI surgery (Figure 6J, and Supplemental Figure 5F). Similar trend was also observed in the EPM and TST paradigm although it did not reach the significance (Figure 6, K and L, and Supplemental Figure 5G). These indicate that RARB regulates neuropathic pain and comorbid anxiodepression via modulation of LAMB1 transcription.

Structural changes of ECM in the CNS are known to be associated with synaptic plasticity and various pathophysiological processes (10, 36). Given the role of LAMB1 as a key element of ECM and a pivotal determinant in chronic pain and comorbid anxiodepression, we were therefore interested in knowing whether this RARB-LAMB1 transcriptional interaction influences the abnormal ECM structural plasticity in the ACC after nerve injury. First, we assessed

whether ECM abnormalities in the ACC occur in response to pain. Following nerve injury, wildtype mice displayed altered ECM microstructure in the ACC, manifesting as thinner and disordered fibers as compared to sham controls (Figure 6, M and N). This ECM abnormalities in microstructure were normalized after overexpression of cingulate RARB (Figure 6, M and N), indicating a crucial role of RARB-LAMB1 signaling in maintaining the stability of ECM microstructure. In further support of this assumption, knockdown of cingulate RARB was shown to provoke the altered ECM microarchitecture in sham mice, which mimics the abnormal ECM structural alterations observed after nerve injury (Figure 6, M and N).

Retinoic acid levels are decreased in patients and mice with chronic pain and comorbid anxiodepression

Retinoic acid acts as an endogenous agonist for RARB, exerting a key role not only in CNS development, but also in regulating synaptic plasticity homeostasis (21-25, 32, 33, 37). Several clinical studies demonstrated the reduced serum RA levels in ischemic stroke patients comorbid with depressive symptoms (38-40), suggesting a negative correlation between RA levels and depressive comorbidities. Then, what changes will occur in RA levels under chronic pain and comorbid anxiodepression? To address this question, we collected 72 blood samples from healthy volunteers and patients with chronic pain. All of them were assessed by pain scale (numerical rating scale, NRS),

depression scale (PHQ-9 and HAMD) and anxiety scale (GAD7 and HAMA), and divided into different groups according to the assessment results (Figure 7A). Interestingly, the serum level of RA from patients with the comorbidity of pain and affective disorders was significantly decreased compared to control group, while that from patients with only pain was not different from controls (Figure 7B). Consistently, lower RA level was also observed in both the serum and ACC in mice at 56 d post-SNI, when pain hypersensitivity and anxiodepression was fully established (Figure 7, C and D). These data indicate that RA metabolic disorder is closely related to anxiodepressive comorbidities associated with pain. To further visualize RA changes, we constructed a GFP-expressing AAV2/9 vector with RA reaction element (RARE) in the promoter, which could be activated by RA to express GFP to achieve RA visualization (Figure 7E). At 24 h after transfection in 293FT cell lines, expression of GFP was stimulated upon application of increasing concentration of RA (Figure 7F). Western blotting analysis verified the elevated GFP expression after RA challenge (Figure 7G). Three weeks after infection with AAV-RARE in the ACC of sham- and SNI-treated mice, immunofluorescence staining revealed that both GFP and RARB expression were significantly lowered after SNI treatment (Figure 7, H and I), further confirming the downregulated RA and RARB after nerve injury. Then, does RA directly regulate RARB expression? To address this question, we constructed luciferase report plasmid containing *Rarb* promoter. Luciferase assay indicated that addition of RA significantly increased

luciferase activity after transfection of *Rarb*-Luc plasmid (Figure 7J). In support of our observation, a previous report has shown that RA specially increases RARB mRNA level in human hepatoma cells (41). Taken together, these results suggest that RA homeostasis is imbalanced and directly affects RARB level in chronic pain state.

Administration of retinoic acid relieves established pain hypersensitivity and anxiodepression after SNI

Finally, we asked whether RA as a kind of vitamin A metabolite has therapeutic effects on neuropathic pain and psychiatric comorbidity. We first delivered RA into ACC at 56 d post-SNI (Figure 8A). Protein levels of LAMB1 and RARB were both upregulated after RA delivery in ACC (Figure 8B). Intracingulate RA delivery dose-dependently inhibited bilateral mechanical allodynia and ipsilateral thermal hyperalgesia induced by SNI (Figure 8, C and D, and Supplemental Figure 6, A-C). In addition, intra-ACC administration of RA increased open-arm exploration in the EPM, enhanced center area traveling in the OFT, decreased the immobility in the TST, and increased sucrose preference at a dose of 50 pmol (Figure 8, E-H, and Supplemental Figure 6, D and E), indicative of anxiolytic and antidepressive effects in the neuropathic state. In contrast, bilateral ACC administration of RA (50 pmol) neither altered basal nociception (Supplemental Figure 6, F-I), nor induced anxiety or depression-like behavior (Supplemental Figure 6, J-M).

Considering potential clinical implication, we further sought to assess the potential analgesic effect of oral RA (Figure 8I). We found that oral intake of RA at 56 d post-SNI significantly alleviated bilateral mechanical allodynia and thermal hyperalgesia (Figure 8, J and K and Supplemental Figure 7, A-C). In addition, the reduced open arm exploring in the EPM, shortened traveling time in the OFT, elongated immobility in the TST as well as reduced sucrose preference in the SPT were all normalized after oral RA delivery in SNI-operated mice (Figure 8, L-O and Supplemental Figure 7, D and E). In contrast, in the basal state, oral administration of RA had no effect on mechanical and thermal threshold, or anxiodepressive behavior (Supplemental Figure 7, F-M). Overall, these results suggest that supplementation of RA via intracingluate injection or oral intake is able to alleviate neuropathic pain and comorbid aversive emotion. Given the systematic effects of oral administration, oral intake of RA may exert analgesic, anxiolytic and antidepressive effects via multiple sites in central and peripheral nervous system. Although we cannot exclude the possible roles of other central and peripheral sites, the essential role of ACC in the beneficial effects of oral RA was established.

We then addressed whether RA relieves neuropathic pain and related anxiodepression via regulating cingulate synaptic plasticity. Bath application of RA (20 μM) reversibly suppressed neuronal hyperexcitability and synaptic transmission of ACC pyramidal neurons in SNI-operated mice, as characterized by reduction of AP frequencies, elevation of AP rheobase and decrease of

AMPARs-eEPSCs (Figure 9, A-F). Furthermore, cingulate long-term potentiation (LTP) induced by pairing training conditioning stimulus was normalized by RA delivery as well (Figure 9, G and H). These results suggest that RA is able to alleviate the abnormal synaptic plasticity. To further confirm whether RA level is modulated by neuronal activity, intra-ACC delivery of TTX (1 μM) and AP5 (100 μM) for 24 h was performed to block APs and NMDA receptors in SNI-treated mice expressing AAV-RARE. Immunofluorescence staining revealed that both GFP and RARB expression were significantly upregulated after administration of TTX and AP5 (Figure 9, I and J), suggesting the modulation of RA by neuronal activity. Taken together, we can infer that RA significantly relieves pain and associated aversion by regulating cingulate synaptic potentiation. Next, we assessed whether RA regulates ECM microstructure via RARB. Following intra-ACC delivery of RA, ECM abnormalities in microstructure after SNI was normalized (Figure 9, K and L). This normalization of dysregulated ECM homeostasis by RA was excluded after knockdown of cingulate RARB (Figure 9, K and L), indicating a vital role of RA in maintaining the stability of ECM microstructure by partially regulating RARB.

Intervention of endogenous RA homeostasis regulates neuropathic pain and pain-related anxiodepression

RA maintains homeostasis through enzyme synthesis and metabolism. RA metabolizing enzyme CYP26 eliminates RA by hydroxylation of polar

metabolites. As a specific CYP26 inhibitor, Talarozole (TLZ) has become a potential therapeutic target by blocking RA metabolism in many fields (27, 42, 43). We then asked whether modulation of endogenous of RA by TLZ alleviates neuropathic pain and related aversion. Intra-ACC delivery of TLZ dose-dependently relieved bilateral mechanical allodynia and ipsilateral thermal hyperalgesia at 56 d after SNI (Figure 10, A-C, and Supplemental Figure 8, A-C). Moreover, bilateral ACC injection of TLZ increased open-arm exploration in the EPM, center area traveling distance in the OFT, struggle time in the TST, and sucrose preference in SNI-operated mice (Figure 10, D-G, and Supplemental Figure 8, D and E), indicative of its desirable anxiolytic and antidepressive effects in the neuropathic state. In contrast, TLZ in ACC rarely affected basal nociception and anxiodepressive behavior (Supplemental Figure 8, F-M). Furthermore, we adopted systemic administration of TLZ via intraperitoneal (i.p.) injection (Figure 10H). In SNI-treated mice, i.p. TLZ significantly alleviated mechanical allodynia and thermal hyperalgesia as well as comorbid anxiodepression in a dose-dependent manner (Figure 10, I-N and Supplemental Figure 9, A-E). In contrast, i.p. TLZ had no effect on the basal nociception (Supplemental Figure 9, F-I). In sum, these results indicate that intervention of endogenous RA metabolism relieves neuropathic pain and related anxiodepression.

For the safety profile study, mice were treated with oral RA for 2 consecutive weeks or i.p. TLZ for consecutive 7 days. The animals showed no changes of

any liver transaminases (ALT and AST) or biomarkers of renal dysfunction (BUN and Creatinine) (Supplemental Figure 10, A-D, F-I). HE staining showed no obvious damage in the lung, liver, kidney and heart of mice treated with chronic RA or TLZ, suggesting that RA and TLZ induced little toxicity in mice (Supplemental Figure 10, E and J).

As mentioned above, synthetase also plays an important role in RA homeostasis. As a key element of RA synthetase, ALDH1A2 is involved in various pathophysiological processes (27, 28, 44). We next generated AAV2/9 expressing ALDH1A2 to explore whether there is a causal relationship between ALDH1A2 and neuropathic pain and anxiodepressive consequences (Supplemental Figure 11A). Western blot analysis revealed that RARB and LAMB1 were both significantly upregulated after ALDH1A2 overexpression (Supplemental Figure 11B). Three weeks after infection of AAV2/9-ALDH1A2, SNI-induced mechanical allodynia and thermal hyperalgesia were significantly relieved compared with control virus (Supplemental Figure 11, C-H). Meanwhile, decreased sucrose preference in the SPT and struggle time in the TST after SNI were largely recovered after overexpressing ALDH1A2 (Supplemental Figure 11, K and L). However, SNI-induced anxiety-like behavior were rarely reversed after ALDH1A2 overexpression (Supplemental Figure 11, I and J). Altogether, it can be inferred that activation of RA synthetase exerts desirable analgesic and antidepressive effects in the neuropathic state, with little anxiolytic effect.

Last, we detected whether RARB in ACC is involved in depression without chronic pain. We used 2 rodent models of depression, one involving chronic exposure to corticosterone (CORT) and the other involving chronic restraint stress (CRS). No significant changes in RARB expression were observed in the ACC after chronic CORT or CRS exposure (Supplemental Figure 12, A and B), suggesting specific involvement of ACC RARB in the development of chronic pain and associated depression but not in non-pain-related depression. Moreover, we found little change in ACC RARB levels in another chronic inflammatory pain model induced by unilateral hindpaw injection of Complete Freund adjuvant (CFA) (Supplemental Figure 12C). Additionally, the changes in ACC RARB levels following SNI were not sex specific, as female mice also showed the downregulated RARB in ACC after SNI (Supplemental Figure 12D). Overall, we can conclude that activation of ACC RA/RARB signaling may represent a potential therapeutic target for treatment of neuropathic pain and related anxiodepression.

Discussion

The results of the present study led us to propose a working model as schematically illustrated in Figure 11. Following nerve injury, enhanced neuronal activity in ACC pyramidal neurons disturbs RA metabolic homeostasis, causing the reduced RA in the ACC. This brings about the downregulation of its corresponding receptor, RARB, which causes a reduction in LAMB1 transcription. This in turn results in disturbance of ECM microstructure, which

further leads to abnormal spine remodeling and synaptic potentiation of ACC pyramidal neurons, collectively contributing to exaggerated pain response and associated anxiodepression. In sum, this study primarily clarifies the role of RA in regulating ECM microstructure by acting on RARB. More importantly, these results infer that maintaining RA homeostasis may be a promising therapeutic strategy for treatment of neuropathic pain and related aversive emotion.

The most striking finding of this study was the identification of RARB, a retinoic acid receptor in the ACC, as a key intracellular upstream trigger for ECM remodeling in regulating neuropathic pain and related anxiodepression. Despite much progress in elucidating the role of ACC in neuropathic pain and comorbid affective disorders, much efforts have been focused on intracellular plasticity, but extracellular alterations have long been overlooked. It is until recently that we uncovered a new mechanism by which a key element of ECM, LAMB1, conveys extracellular alterations to intracellular structural and functional plasticity and thus underlies neuropathic pain and anxiodepressive consequences (11). However, it remains elusive what triggers activity-dependent changes of LAMB1 and further ECM remodeling after nerve injury. Using RNA-seq, we detected 10 differential changes of transcription factors related with *Lamb1* in the ACC after SNI treatment. It is noteworthy that amongst which, RARB showed stronger association with *Lamb1*. As a nuclear receptor superfamily, retinoic acid receptors (RARs), consisting of α, β and γ subunits (13, 19), are assumed to function as transcription factors by binding to

the RARE in the promoters of target genes, which is involved in neuronal development, synaptic plasticity and homeostasis, ultimately affecting multiple brain functions, i.e. learning, memory and affective cognition (13, 16, 18, 19, 45). In support of our observation, *in vitro* studies using murine and human cell lines identified a RARE in the 5′-flanking region of *Lamb1* gene and reported a preferential binding of RARB to the RARE of *Lamb1* promoter and triggering *Lamb1* gene transcription (12, 17). However, it remains unclear whether RARB regulates transcription of LAMB1 in the ACC and how this transcriptional interaction contributes to the development of neuropathic pain and comorbid anxiodepression. Consistent with downregulated LAMB1 as reported previously (11), we verified similar downregulation of RARB at transcriptional, mRNA and protein levels after SNI. Western blotting analysis showed that overexpression or knockdown of RARB in the ACC correspondingly leads to upregulation or downregulation of LAMB1 expression. Luciferase and ChIP assay further demonstrated the transcription-promoting capacity of potential RARB-binding sites in *Lamb1* genes. These data suggest that RARB may act as an upstream transcription factor for LAMB1 in the ACC.

It is well known that structural changes of ECM in the CNS are associated with synaptic plasticity and various pathophysiological processes (10, 36). Given the role of LAMB1 as a key element of ECM and a pivotal determinant in chronic pain and comorbid anxiodepression, an interesting question arises regarding whether this RARB-LAMB1 signaling influences abnormal structural

plasticity of ECM in the ACC after nerve injury. In the present study, we demonstrated that nerve injury induces altered ECM microstructure in the ACC, which was normalized after overexpression of cingulate RARB, indicating a crucial role of RARB-LAMB1 signaling in maintaining the stability of ECM microstructure.

To further determine the causal relationship between plastic changes of cingulate RARB and neuropathic pain, we overexpressed RARB in the ACC and found that supplementation of RARB significantly alleviated pain hypersensitivity and related anxiety and depression in SNI-treated mice. In contrast, knocking down cingulate RARB exaggerated pain sensitivity and induced anxiodepression in control mice. More importantly, the above actions of RARB were excluded by blockade of LAMB1. Thus, we can infer that RARB in the ACC may negatively regulate neuropathic pain and anxiodepressive consequences via regulation of LAMB1 transcription. Additionally, we found no sex difference in the role of cingulate RARB on neuropathic pain and affective disorders. In contrast, RARB in the ACC may not be involved in depression with no pain, since we found no significant alteration of cingulate RARB in rodent models of chronic CORT and CRS exposure. These results are consistent with changes in ACC LAMB1 in our previous study (11). In support of this assumption, previous studies have shown an increased RARA and its transcriptional regulation of corticotrophin-releasing hormone (CRH) gene expression in the paraventricular nucleus (PVN) in patients with affective

disorders (46). A reduced level of RARA and its transcriptional target gene TrkB has been reported in the dorsolateral prefrontal cortex of elderly depressed patients (47). These data indicate that depression comorbid with neuropathic pain and depression without pain may involve different types of RARs and transcriptional regulation of different target genes in different brain regions. Additionally, RARB in the hippocampus was reported to be associated with learning and memory (19, 45).

Then how does RARB in the ACC accomplish regulation of neuropathic pain and comorbid anxiodepression? Structural and functional plasticity in the ACC is assumed to be a cellular basis for neuropathic pain and associated anxiodepression (5-8). Emerging evidence has documented the key significance of RARs signaling in synaptic transmission, homeostatic synaptic plasticity in many brain regions, i.e. hippocampus (19, 30, 48, 49), somatosensory cortex (50), visual cortex (51), spinal cord (52), etc. Another intriguing finding of this study entails the contribution of RARB to the ACC in negatively orchestrating cingulate structural and functional plasticity. In the present study, we observed that overexpression of cingulate RARB normalized abnormal spine remodeling after SNI. These results confirm that RARB plays a pivotal role in synaptic spine stabilization in ACC pyramidal neurons. Functional synaptic plasticity is closely related to synaptic spine remodeling, both of which collectively contribute to various pathophysiological processes, including chronic pain (53). Consistent with spine remodeling, patch-clamp recordings

revealed that overexpression of RARB significantly relieved SNI-induced hyperexcitability and AMPAR-mediated synaptic potentiation in ACC pyramidal neurons. Further mechanistic analysis revealed that both pre- and post-synaptic mechanisms were involved in the above-described synaptic modulation by RARB. This crucial role of RARB on cingulate functional plasticity was further strengthened with alternative *in vivo* evidence by using fiber photometry recording. GCaMP6s-based imaging showed that overexpression of ACC RARB inhibited photometric Ca^{2+} transients of ACC pyramidal neurons in response to peripheral stimuli as well as tail suspension after SNI, while knockdown of cingulate RARB sensitized Ca^{2+} responses. Overall, we can infer that exogenous supplementation of RARB was able to normalize abnormal structural and functional plasticity of ACC pyramidal neurons after peripheral neuropathy, which in turn produced analgesic, anxiolytic and antidepressive effects.

Exactly how RARB as a nuclear receptor is regulated upon nerve injury and further modulates neuropathic pain and related anxiodepression is not entirely understood. Another striking finding of this study is that we revealed the involvement of activity-dependent dysregulation of retinoic acid (RA) homeostasis in the above process. Mounting evidence has shown that RA functions as an endogenous ligand for nuclear RARs to directly regulate genomic transcription (28, 54, 55). RA is a metabolic product of vitamin A. Early studies regarding vitamin A and RA have been mainly focusing on the eye, skin,

immune and reproductive systems (15, 28, 29). However, emerging studies showed that controlled RA synthesis is essential for regulating synaptic plasticity and homeostasis, and RA deficiency is closely associated with several psychiatric and developmental disorders and cognitive dysfunction (21, 30, 32, 56, 57). Several clinical studies have inferred that reduced vitamin A or RA level is related to higher risk of depression in patients with ischemic stroke and solvent-induced neuropathy, while supplementation of vitamin A or RA is inversely associated with depression and sensory abnormality (39, 58, 59). However, it remains unknown whether RA homeostasis is disturbed under neuropathic pain states comorbid with affective disorders. Interestingly, using ELISA assay we observed a significantly lower RA level in the serum in patients with neuropathic pain and related anxiodepression as compared to healthy controls. Consistently, the reduced RA level was also seen in both the serum and ACC in SNI-injured mice with pain hypersensitivity and anxiodepression. These data indicate that dysregulated RA homeostasis in ACC is closely related to depressive comorbidities associated with chronic pain.

Then what causes dysregulated RA homeostasis after nerve injury? It is well established that RA plays an important role in homeostatic synaptic plasticity (30, 31, 60). Neuronal activity blockade-which induces homeostatic plasticity-strongly stimulates RA synthesis in neurons and rapidly enhances synaptic strength (30). In addition to homeostatic plasticity, RA signaling is also involved in multiple forms of synaptic plasticity, i.e. LTP and/or LTD (19, 61, 62). In the

present study, we observed that blockade of cingulate neuronal activity with TTX and AP5 reversed the reduction of RA level in ACC after nerve injury. This suggests that the reduced RA level after nerve injury might be partly dependent on neuronal hyperactivity in ACC. Nevertheless, we cannot exclude the possible contribution of peripheral RA depletion in ACC RA reduction after nerve injury. It remains to be further investigated regarding the relative contributions of central *vs* systemic RA signaling to pain and affective comorbidities. Further mechanistic analysis demonstrated that RA synthesis is Ca^{2+}-dependent, that is, in synaptically active neurons, modest “basal” levels of postsynaptic Ca^{2+} physiologically suppress RA synthesis, whereas in synaptically inactive neurons, decreases in the resting Ca^{2+} levels induce homeostatic plasticity by stimulating synthesis of RA that then acts in a cell-autonomous manner to increase AMPA receptor function (63). In the present study, given our observation that intracellular Ca^{2+} level in cingulate pyramidal neurons gets increased significantly after nerve injury, this suggests that the reduced RA level observed in patients and mice with chronic pain and comorbid affective disorders might result from further suppression of RA synthesis by exaggerated Ca^{2+} level.

Considering the dysregulated RA homeostasis after nerve injury, we thought that rectifying this dysregulation would produce beneficial effects on neuropathic pain and comorbid affective disorders. In support of this assumption, we provided three lines of evidence. First, direct exogenous

supplementation of RA via different route of administration, i.e. intracingulate injection and oral delivery, had a strong ability to relieve SNI-induced pain hypersensitivity and anxiodepression. Further mechanistic analysis revealed that this analgesic as well as anxiolytic and antidepressive effects are achieved by suppression of pyramidal neuronal hyperexcitability after SNI. Second, intervention of endogenous RA homeostasis was able to improve neuropathic pain and related anxiodepression. It is well known that RA maintains homeostasis *in vivo* through enzyme synthesis and metabolism (28). The RA metabolizing enzyme CYP26 eliminates RA by hydroxylation of polar metabolites (42, 43). Talarozole (TLZ), a specific CYP26 inhibitor, has been widely used in clinic and shown potential therapeutic effects in several diseases by blocking RA metabolism (27, 42, 43). Here, our results extended a new role of TLZ in treatment of neuropathic pain and related affective disorders. Systemic or intracingulate administration of TLZ showed potent efficacy in alleviating pain hypersensitivity and anxiodepression in the neuropathic state. In parallel, enhancing endogenous RA synthetase by overexpression of ALDH1A2 in the ACC exerted desirable analgesic and antidepressive effects. These lines of evidence collectively indicate that daily supplementation of RA or vitamin A may be beneficial for pain relief and mood improvement after nerve injury. Nevertheless, there are also evidence linking RA signaling and depression-like behaviors, which showed that long-term use of high-dose isotretinoin in patients with acne treatment has potential risk of depression, and

the mechanism may be related to activation of HPA axis (29, 38, 64, 65). On the other hand, some studies point the opposite view that acne causes depression and that treatment leads to an improvement in depression (29, 66, 67). Overall, there is no consistent evidence to prove the relationship between isotretinoin and affective disorders after patients with acne treatment.

In summary, this study shows how cingulate RA/RARB homeostasis modulates neuropathic pain and associated anxiodepression via interaction with ECM LAMB1. Taken together with our previous study in which ECM LAMB1 conveys extracellular alterations to intracellular structural and functional plasticity (11), we revealed an intracellular-extracellular-intracellular feedforward regulatory network underlying the comorbidity of neuropathic pain and anxiodepression. Namely, nerve injury induces dysregulated RA homeostasis and subsequent downregulated RARB/LAMB1 transcriptional signaling (intracellular), which leads to ECM abnormalities in microstructure (extracellular) and further triggers the abnormal structural and functional plasticity via intracellular signaling cascades (intracellular), ultimately resulting in pain chronicity and related affective disorders. Moreover, our results imply that RA may act as a potential indicator for the comorbidity of neuropathic pain and affective disorders and present a promising therapeutic target for treatment of this disorder.

Methods

Sex as a biological variable

Sex was not considered as a biological variable.

Animals

Adult C57BL/6 mice (6-8 weeks old) were used in all experiments except for patch-clamp recording experiments (4-5 weeks old mice), and raised under a temperature-controlled environment with a 12 h light-dark cycle. Except for the detection of RARB level after SNI injury with both sexes of mice, all the other experiments used male mice. All tests were done in a double-blinded manner.

Animal models

Spared nerve injury surgery. Spared nerve injury (SNI) model is a well-established model of peripheral nerve injury as previously described (11). See Supplemental methods for details.

Chronic CORT and CRS model. See Supplemental methods for details.

Chronic inflammatory pain model. Unilateral injection of complete Freund's adjuvant (CFA) (20 μl) was performed into the intraplantar surface of mouse hindpaw, as described previously (11).

Clinical studies

Human serum samples. Seventy-two blood samples from patients and healthy

volunteers were collected within 1 year. The blood samples were collected from inpatient patients with chronic pain in the rehabilitation department in Xijing hospital. See Supplemental methods for the clinical samples collection criteria in details.

Grouping of blood samples. All the participants were further assessed by pain scale (numerical rating scale, NRS), depression scale (PHQ-9 and HAMD) and anxiety scale (GAD7 and HAMA), and divided into different groups according to the assessment results.

Retinoic acid level detection

The collected blood samples from human and mice were all centrifuged at 1000×g for 10 min. Serums were obtained and stored at -80°C. Retinoic acid level test using Human Retinoic acid ELISA kit (CSB-E16712h, CUSABIO, Wuhan, China) and Mouse Retinoic acid ELISA kit (CSB-EQ028019MO, CUSABIO) separately in accordance with the manufacturer's protocol.

Transcription factor prediction

The potential transcription factors with significant difference of *Lamb1* were further analyzed according to previous RNA-seq data (Gene Denovo Biotechnology) (11).

Real-time PCR, western blotting and immunofluorescent staining

See the Supplemental methods for details.

Stereotaxic surgery

See the Supplemental Methods for details.

Behavioral analyses

All mice were allocated randomly in experimental group. Before behavioral tests, mice were allowed to acclimatize to behavioral testing room for 1 d and performed in a blinded manner. Mechanical stimulation threshold was assessed by von Frey hairs to the planter surface. Thermal stimulation latency was assessed by a radiant heat source applied to the plantar surface. Anxiodepressive-like behaviors were analyzed by EPM, OFT, TST and SPT paradigms. See the Supplemental Methods for detailed procedures.

Golgi staining

See the Supplemental Methods for details.

Electrophysiology

Whole-cell patch-clamp recording was performed as described previously (11). The electrophysiological properties of the recorded neurons were acquired with an Axon700B amplifier (Molecular Devices Corporation, CA, USA) and pCLAMP10.0 software. The input-output of AMPAR-mediated eEPSCs were

recorded from layer II/III neurons, and the stimulations were delivered by a field stimulating electrode placed in layer V/VI of the ACC. Paired-pulse ratio of AMPARs-mediated eEPSCs was calculated as the amplitude of the second eEPSCs divided by that of the first eEPSCs in a pair. For membrane properties analysis, depolarizing current steps (500 ms in duration and 20 pA increments) were used to detect the AP under current-clamp mode. Miniature EPSCs (mEPSCs) were recorded at a holding potential of -70 mV in the presence of AP5 (50 μM), picrotoxin (100 μM) and tetrodotoxin (TTX) (0.5 μM). Long-term potentiation (LTP) was induced by 80 paired presynaptic pulses at 2 Hz coupled with postsynaptic depolarization at +30 mV, as reported previously (68). See the Supplemental Methods for details.

Calcium imaging

Fiber photometry was used to record calcium dependent activity dynamics during behavioral test with the commercialized fiber photometry system (ThinkerTech, Beijing, China) as described previously (11). See the Supplemental Methods for details.

Dual-Lucy Assay

293FT cell line (Invitrogen, R70007) was transfected with plasmid mixture of luciferase reporter vector, transcription factor plasmid and Renilla luciferases vector (10:9:1) using Lipofectamine 3000 kit (L3000075, Invitrogen). At 48 h

after transfection, luciferase test was measured by Dual-Lucy Assay kit (D0010, Solarbio) in accordance with the manufacturer's protocol. The final results were normalized to Renilla luciferase activity.

Chromatin immunoprecipitation (ChIP)

See the Supplemental methods for details.

Scanning electron microscopy

Mice were anesthetized with isoflurane and transcardially perfused with ice-cold PBS. Coronal slices (1.5 mm-thickness) containing the injected ACC were prepared and decellularized as previously described (69). Briefly, the obtained slices were performed consisting of three cycles using demineralized water, sodium deoxycholate (D8331, Solarbio), DNase I (D8071, Solarbio) diluted in 1 M NaCl solution and Triton X-100. Then, the decellularized slices were fixed with glutaraldehyde at 4°C for 24 h. The samples were rinsed in dH_2O and gradually dehydration in gradient increasing concentrations of ethanol. Samples were then stacked horizontally on a wire mesh divider to keep them flat and dried using the hexamethyl disilazane (283134, Sigma-Aldrich) about 30 min. The dried samples were mounted on an Aluminum SEM rod with a conductive copper tape and sputtered coating, then imaged with Hitachi S-4800 (Tokyo, Japan) using InLens SE at an operating voltage of 5 KV. ECM fiber diameter was analyzed using Image J.

Rescue experiments

Intracingulate drug delivery. The ACC of mice were implanted with bilateral 26 gauge (Ga) stainless steel guide cannula (0.8 mm separation, RWD Life Science) according to the above coordinates. See the Supplemental methods for details.

Systemic administration. See the Supplemental methods for details.

Statistical analysis

Data were analyzed in GraphPad Prism version 8.0 (GraphPad Software, La Jolla, CA, USA) and Statistical Program for Social Sciences 21.0 software (SPSS, Inc., Chicago, IL, USA). The normality test was performed by the Shapiro–Wilk test. The homogeneity of variance test was performed by Levene's test. Data that met these two conditions were analyzed using a 2-tailed unpaired or paired *t* test, 1-way analysis of variance (ANOVA) and 2-way ANOVA followed by Tukey's multiple comparisons test or Dunnett's multiple comparisons test. Data sets that were not normally distributed were analyzed with a nonparametric test (Supplemental Table 2). Data are reported as mean ± standard error of the mean. *P* value less than 0.05 was considered statistically significant.

Study approval

All animal procedures were reviewed and approved by Institutional Animal Care and Use Committee of the Fourth Military Medical University (FMMU). All clinical samples have been conducted according to Declaration of Helsinki principles, approved within the Medical Ethics of the First Affiliated Hospital of Fourth Military Medical University (Ethics Committee approval number: KY20232185-F-1) and Chinese Clinical Trial Registry (Registration No. ChiCTR2300076022). All participants have read and signed the informed consents prior to inclusion in the study. All testing was done in a double-blinded manner, and consent was received from participants.

Data availability

RNA-seq data have been deposited in the National Center for Biotechnology Information Sequence Red Archive (SRA) under the accession code SRP323752. Values for all data points in graphs are reported in the Supporting Data Values file. The data generated in this study are available upon request from the corresponding authors.

Author contributions

ZZL, WNL, KXL and ZWD performed animal preparation. ZZL designed and performed RNA-sequencing analysis. ZZL, WNL and KXL conducted western blotting. ZZL, FW, WJH and RGX performed brain slice patch clamp recording. ZZL, XLS, HY and RZ designed and conducted clinical trials. KXL, ZWD and

YC performed and analysed the Golgi staining. WNL, ZWD and KXL performed immunofluorescence staining. ZZL, WNL and RZ performed SEM, Dual-Lucy assay and Retinoic acid level detection. ZZL, WNL, KXL, TZW and WGC conducted behavioural and pharmacological testing. ZZL, WNL, KXL and MMW conducted stereotaxic surgery and fiber photometry. ZZL, KXL and XXZ analysed data. CL, SXW, ZZL, XFJ and XLS designed studies, CL and ZZL wrote the draft manuscript. CL, SXW and ZZL supervised the experiments and revised the manuscript. All the authors read and approved the final manuscript.

Acknowledgements

We thank the colleagues from rehabilitation department in Xijing hospital, Xiao-Dong Lin, Lin-Na Hui and Fang-Fang Liu, for help with collection of information and blood samples from volunteers. This work was supported by Natural Science Foundation of China (NSFC) grants to S.X.W. (82221001); STI2030-Major Projects to C. L. (2021ZD0203100 (2021ZD0203104)); NSFC grants to Z.Z.L. (82201368), to C.L. (82330036, 32071002), to F.W (82201370), to W.J.H. (82101293); National Key Research and Development Program of China to C.L. (2024YFC2510102); China Postdoctoral Science Foundation grant to Z.Z.L (2022M713847, 2023T160779), to F.W. (2021MD703955); grant from Innovation Team Accredited by Shaanxi Science and Technology to C.L. (2022TD-49); grant from Joint Founding Project of Innovation Research Institute, Xijing Hospital (LHJJ24JH08) and Shaanxi Province Sanqin Talent

Program to C.L.

REFERENCES

1. Bushnell MC, et al. Cognitive and emotional control of pain and its disruption in chronic pain. *Nat Rev Neurosci.* 2013;14(7):502-11.
2. Barthas F, et al. The anterior cingulate cortex is a critical hub for pain-induced depression. *Biol Psychiatry.* 2015;77(3):236-45.
3. Vogt BA. Pain and emotion interactions in subregions of the cingulate gyrus. *Nat Rev Neurosci.* 2005;6(7):533-44.
4. Meng F, et al. Neural mechanisms of social empathy in the anterior cingulate cortex. *AN.* 2023;2(1).
5. Bliss TV, et al. Synaptic plasticity in the anterior cingulate cortex in acute and chronic pain. *Nat Rev Neurosci.* 2016;17(8):485-96.
6. Koga K, et al. Coexistence of two forms of LTP in ACC provides a synaptic mechanism for the interactions between anxiety and chronic pain. *Neuron.* 2015;85(2):377-89.
7. Zhuo M. Neural Mechanisms Underlying Anxiety-Chronic Pain Interactions. *Trends Neurosci.* 2016;39(3):136-45.
8. Sellmeijer J, et al. Hyperactivity of Anterior Cingulate Cortex Areas 24a/24b Drives Chronic Pain-Induced Anxiodepressive-like Consequences. *J Neurosci.* 2018;38(12):3102-15.
9. Archibald J, et al. Metabolite activity in the anterior cingulate cortex during a painful stimulus using functional MRS. *Sci Rep.* 2020;10(1):19218.
10. Dityatev A, et al. The dual role of the extracellular matrix in synaptic

plasticity and homeostasis. *Nat Rev Neurosci.* 2010;11(11):735-46.

11. Li ZZ, et al. Extracellular matrix protein laminin beta1 regulates pain sensitivity and anxiodepression-like behaviors in mice. *J Clin Invest.* 2021;131(15).
12. Vasios GW, et al. A retinoic acid-responsive element is present in the 5' flanking region of the laminin B1 gene. *Proc Natl Acad Sci U S A.* 1989;86(23):9099-103.
13. Hashimoto Y. Retinobenzoic acids and nuclear retinoic acid receptors. *Cell Struct Funct.* 1991;16(2):113-23.
14. Mic FA, et al. Retinoid activation of retinoic acid receptor but not retinoid X receptor is sufficient to rescue lethal defect in retinoic acid synthesis. *Proc Natl Acad Sci U S A.* 2003;100(12):7135-40.
15. Das BC, et al. Retinoic acid signaling pathways in development and diseases. *Bioorg Med Chem.* 2014;22(2):673-83.
16. Goncalves MB, et al. RARbeta Agonist Drug (C286) Demonstrates Efficacy in a Pre-clinical Neuropathic Pain Model Restoring Multiple Pathways via DNA Repair Mechanisms. *iScience.* 2019;20:554-66.
17. Vasios G, et al. The late retinoic acid induction of laminin B1 gene transcription involves RAR binding to the responsive element. *EMBO J.* 1991;10(5):1149-58.
18. Ciancia M, et al. Retinoic acid receptor beta protects striatopallidal medium spiny neurons from mitochondrial dysfunction and neurodegeneration.

Prog Neurobiol. 2022;212:102246.

19. Chiang MY, et al. An essential role for retinoid receptors RARbeta and RXRgamma in long-term potentiation and depression. *Neuron.* 1998;21(6):1353-61.
20. Bianchi MG, et al. The ATRA-dependent overexpression of the glutamate transporter EAAC1 requires RARbeta induction. *Biochim Biophys Acta.* 2009;1788(9):1861-8.
21. Woloszynowska-Fraser MU, et al. Vitamin A and Retinoic Acid in Cognition and Cognitive Disease. *Annu Rev Nutr.* 2020;40:247-72.
22. Kouchmeshky A, and McCaffery P. Use of fixatives for immunohistochemistry and their application for detection of retinoic acid synthesizing enzymes in the central nervous system. *Methods Enzymol.* 2020;637:119-50.
23. Hu P, et al. Retinoic acid and depressive disorders: Evidence and possible neurobiological mechanisms. *Neurosci Biobehav Rev.* 2020;112:376-91.
24. Wallace JL, and Pollen AA. The genetic symphony underlying evolution of the brain's prefrontal cortex. *Nature.* 2021;598(7881):417-8.
25. Shibata M, et al. Regulation of prefrontal patterning and connectivity by retinoic acid. *Nature.* 2021;598(7881):483-8.
26. Lane MA, and Bailey SJ. Role of retinoid signalling in the adult brain. *Prog Neurobiol.* 2005;75(4):275-93.
27. Zhu L, et al. Variants in ALDH1A2 reveal an anti-inflammatory role for

retinoic acid and a new class of disease-modifying drugs in osteoarthritis. *Sci Transl Med.* 2022;14(676):eabm4054.

28. Ghyselinck NB, and Duester G. Retinoic acid signaling pathways. *Development.* 2019;146(13).
29. Bremner JD, et al. Retinoic acid and affective disorders: the evidence for an association. *J Clin Psychiatry.* 2012;73(1):37-50.
30. Aoto J, et al. Synaptic signaling by all-trans retinoic acid in homeostatic synaptic plasticity. *Neuron.* 2008;60(2):308-20.
31. Arendt KL, et al. Retinoic Acid and LTP Recruit Postsynaptic AMPA Receptors Using Distinct SNARE-Dependent Mechanisms. *Neuron.* 2015;86(2):442-56.
32. Reay WR, et al. Polygenic disruption of retinoid signalling in schizophrenia and a severe cognitive deficit subtype. *Mol Psychiatry.* 2020;25(4):719-31.
33. Zhou W, and Li S. Decreased levels of serum retinoic acid in chinese children with autism spectrum disorder. *Psychiatry Res.* 2018;269:469-73.
34. Tsvetkov E, et al. Fear conditioning occludes LTP-induced presynaptic enhancement of synaptic transmission in the cortical pathway to the lateral amygdala. *Neuron.* 2002;34(2):289-300.
35. Schulz PE, et al. Using paired-pulse facilitation to probe the mechanisms for long-term potentiation (LTP). *J Physiol Paris.* 1995;89(1):3-9.
36. Tajerian M, et al. The hippocampal extracellular matrix regulates pain and memory after injury. *Mol Psychiatry.* 2018;23(12):2302-13.

37. Xu X, et al. Excessive UBE3A dosage impairs retinoic acid signaling and synaptic plasticity in autism spectrum disorders. *Cell Res.* 2018;28(1):48-68.
38. Al-Fartusie FS, et al. Evaluation of Some Trace Elements and Vitamins in Major Depressive Disorder Patients: a Case-Control Study. *Biol Trace Elem Res.* 2019;189(2):412-9.
39. Yang CD, et al. Association of serum retinoic acid with depression in patients with acute ischemic stroke. *Aging (Albany NY).* 2020;12(3):2647-58.
40. Zhang Y, et al. Associations of Dietary Vitamin A and Beta-Carotene Intake With Depression. A Meta-Analysis of Observational Studies. *Front Nutr.* 2022;9:881139.
41. de The H, et al. Differential expression and ligand regulation of the retinoic acid receptor alpha and beta genes. *EMBO J.* 1989;8(2):429-33.
42. Cao DL, et al. Cytochrome P450 26A1 Contributes to the Maintenance of Neuropathic Pain. *Neurosci Bull.* 2024;40(3):293-309.
43. Stevison F, et al. Inhibition of the all-trans Retinoic Acid (atRA) Hydroxylases CYP26A1 and CYP26B1 Results in Dynamic, Tissue-Specific Changes in Endogenous atRA Signaling. *Drug Metab Dispos.* 2017;45(7):846-54.
44. Goncalves MB, et al. Retinoic acid synthesis by NG2 expressing cells promotes a permissive environment for axonal outgrowth. *Neurobiol Dis.*

2018;111:70-9.

45. Nomoto M, et al. Dysfunction of the RAR/RXR signaling pathway in the forebrain impairs hippocampal memory and synaptic plasticity. *Mol Brain.* 2012;5:8.

46. Chen XN, et al. The involvement of retinoic acid receptor-alpha in corticotropin-releasing hormone gene expression and affective disorders. *Biol Psychiatry.* 2009;66(9):832-9.

47. Qi XR, et al. Abnormal retinoid and TrkB signaling in the prefrontal cortex in mood disorders. *Cereb Cortex.* 2015;25(1):75-83.

48. Hsu YT, et al. Synaptic retinoic acid receptor signaling mediates mTOR-dependent metaplasticity that controls hippocampal learning. *Proc Natl Acad Sci U S A.* 2019;116(14):7113-22.

49. Sarti F, et al. Rapid suppression of inhibitory synaptic transmission by retinoic acid. *J Neurosci.* 2013;33(28):11440-50.

50. Park E, et al. Postnatal Ablation of Synaptic Retinoic Acid Signaling Impairs Cortical Information Processing and Sensory Discrimination in Mice. *J Neurosci.* 2018;38(23):5277-88.

51. Zhong LR, et al. Retinoic Acid Receptor RARalpha-Dependent Synaptic Signaling Mediates Homeostatic Synaptic Plasticity at the Inhibitory Synapses of Mouse Visual Cortex. *J Neurosci.* 2018;38(49):10454-66.

52. Cao B, et al. Spinal cord retinoic acid receptor signaling gates mechanical hypersensitivity in neuropathic pain. *Neuron.* 2022;110(24):4108-24 e6.

53. Kuner R, and Flor H. Structural plasticity and reorganisation in chronic pain. *Nat Rev Neurosci.* 2017;18(2):113.
54. Chambon P. A decade of molecular biology of retinoic acid receptors. *FASEB J.* 1996;10(9):940-54.
55. Cunningham TJ, and Duester G. Mechanisms of retinoic acid signalling and its roles in organ and limb development. *Nat Rev Mol Cell Biol.* 2015;16(2):110-23.
56. Luo T, et al. Integrating retinoic acid signaling with brain function. *Dev Psychol.* 2009;45(1):139-50.
57. Xu D, et al. WDR62-deficiency Causes Autism-like Behaviors Independent of Microcephaly in Mice. *Neurosci Bull.* 2023;39(9):1333-47.
58. Hu B, et al. Dietary Zinc Intake Affects the Association Between Dietary Vitamin A and Depression: A Cross-Sectional Study. *Front Nutr.* 2022;9:913132.
59. Hamed EA, et al. Role of monocyte chemoattractant protein-1, stromal derived factor-1 and retinoic acid in pathophysiology of neuropathic pain in rats. *J Basic Clin Physiol Pharmacol.* 2016;27(4):411-24.
60. Lenz M, et al. All-trans retinoic acid induces synaptic plasticity in human cortical neurons. *Elife.* 2021;10.
61. Misner DL, et al. Vitamin A deprivation results in reversible loss of hippocampal long-term synaptic plasticity. *Proc Natl Acad Sci U S A.* 2001;98(20):11714-9.

62. Cocco S, et al. Vitamin A deficiency produces spatial learning and memory impairment in rats. *Neuroscience.* 2002;115(2):475-82.
63. Wang HL, et al. Decrease in calcium concentration triggers neuronal retinoic acid synthesis during homeostatic synaptic plasticity. *J Neurosci.* 2011;31(49):17764-71.
64. Bremner JD, and McCaffery P. The neurobiology of retinoic acid in affective disorders. *Prog Neuropsychopharmacol Biol Psychiatry.* 2008;32(2):315-31.
65. Hu P, et al. All-trans retinoic acid-induced hypothalamus-pituitary-adrenal hyperactivity involves glucocorticoid receptor dysregulation. *Transl Psychiatry.* 2013;3(12):e336.
66. Schrom K, et al. Depression screening using health questionnaires in patients receiving oral isotretinoin for acne vulgaris. *J Am Acad Dermatol.* 2016;75(1):237-9.
67. Acne, isotretinoin and depression. *Drug Ther Bull.* 2003;41(10):76-8.
68. Guo B, et al. Anterior cingulate cortex dysfunction underlies social deficits in Shank3 mutant mice. *Nat Neurosci.* 2019;22(8):1223-34.
69. De Waele J, et al. 3D culture of murine neural stem cells on decellularized mouse brain sections. *Biomaterials.* 2015;41:122-31.

Figure legends

Figure 1 Peripheral neuropathy decreases RARB expression in the ACC. (A) Potential transcription factors of *Lamb1* with differentially expressed genes in RNA-seq data of contralateral ACC from SNI- *vs* sham-treated mice. The line color and size are defined as the relativity with the *Lamb1*. (n = 3-4 mice per group). (B, C) RARB expression in the ACC after SNI surgery at both mRNA (B) (n = 3) and protein level (C) (n = 3). (D, E) Representative examples (D) and quantitative summary (E) of RARB co-expressing with NeuN, GFAP or Iba1 (n = 3). (F, G) Representative examples (F) and quantitative summary (G) of RARB co-expressing with CaMKII or GAD67 neurons (n = 3). Scale bar: 30 μm in (D) and (F). *P < 0.05, **P < 0.01. Statistical analysis was performed by 1-way ANOVA (B, and C for RARB / GAPDH) and Kruskal-Wallis H test (C for RARA / GAPDH).

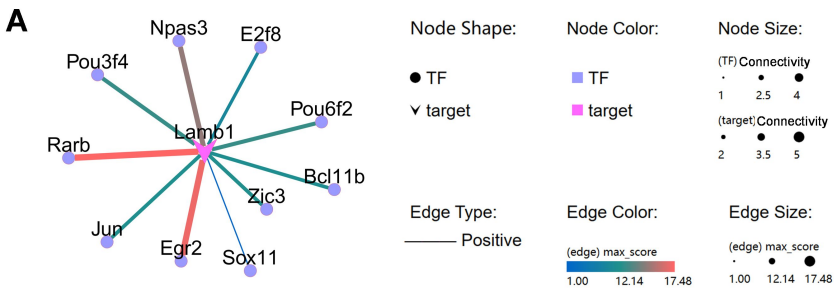
A
Npas3
E2f8
Pou3f4
Pou6f2
Rarb
Lamb1
Bcl11b
Zic3
Jun
Egr2
Sox11
Node Shape:
TF
target
Node Color:
TF
target
Node Size:
(TF) Connectivity
1
2.5
4
(target) Connectivity
2
3.5
5
Edge Type:
Positive
Edge Color:
(edge) max_score
1.00
12.14
17.48
Edge Size:
(edge) max_score
1.00
12.14
17.48

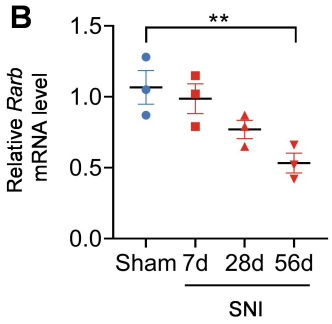
B
Relative Rarb mRNA level
1.5
1.0
0.5
0.0
**
Sham
7d
28d
56d
SNI

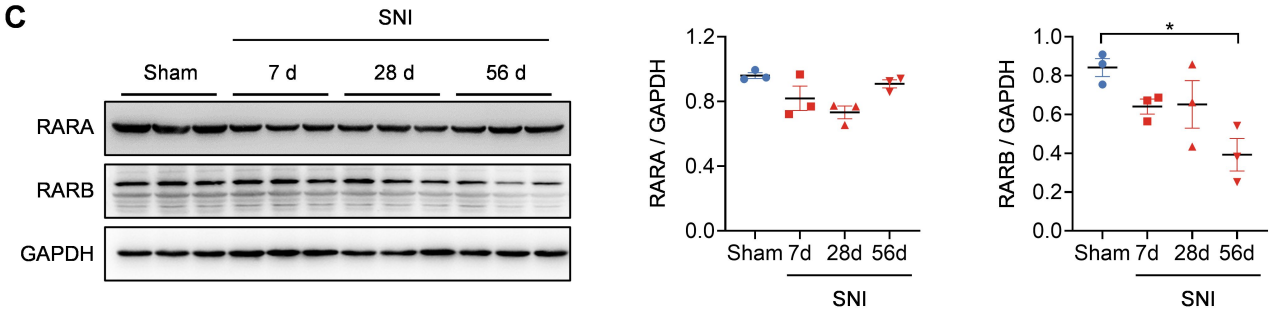
C
SNI
Sham
7 d
28 d
56 d
RARA
RARB
GAPDH
RARA / GAPDH
1.2
0.8
0.4
0.0
Sham 7d 28d 56d
SNI
RARB / GAPDH
1.0
0.8
0.6
0.4
0.2
0.0
*
Sham 7d 28d 56d
SNI

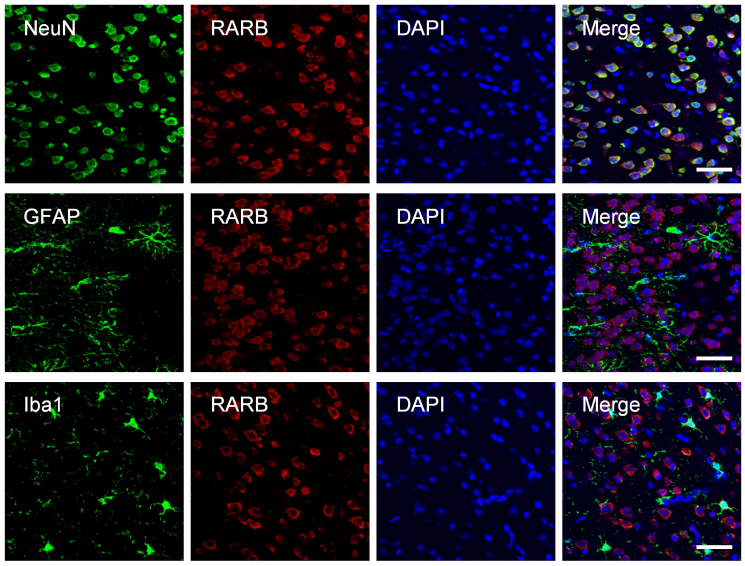
D
NeuN
RARB
DAPI
Merge
GFAP
RARB
DAPI
Merge
Iba1
RARB
DAPI
Merge

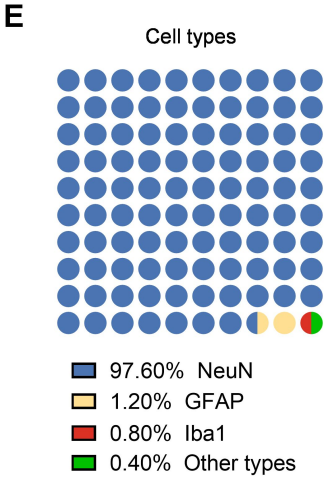
E
Cell types
97.60% NeuN
1.20% GFAP
0.80% Iba1
0.40% Other types

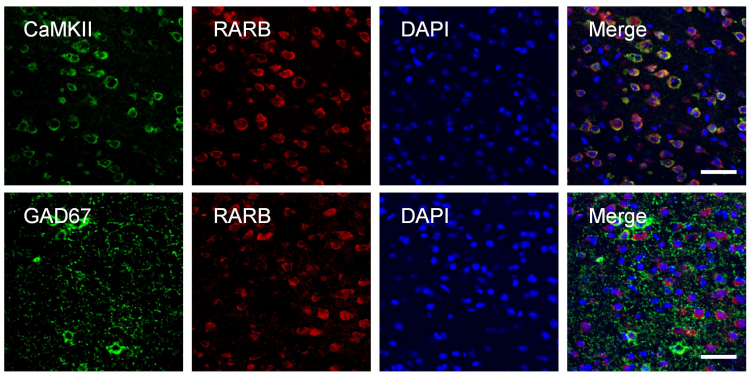
F
CaMKII
RARB
DAPI
Merge
GAD67
RARB
DAPI
Merge

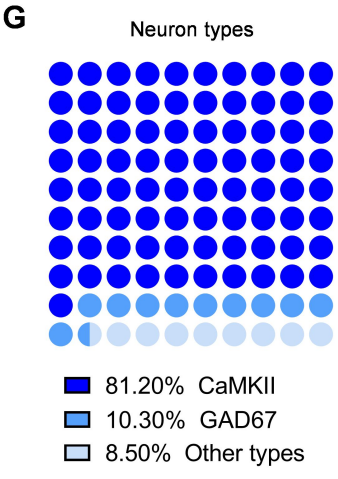
G
Neuron types
81.20% CaMKII
10.30% GAD67
8.50% Other types

Figure 2 RARB overexpression in ACC relieves pain hypersensitivity and anxiodepression. (A) Schematic diagram showing intra-ACC virus injection. Scale bars: 1 mm (enlarged insets). (B, C) Double immunofluorescence (B) and western blotting (C) showing efficient RARB overexpression in ACC (n = 4). Scale bar: 30 μm in (B). (D) Experimental schematic diagram showing virus injection in ACC and behavioral test. (E, F) Ipsilateral stimulus-response curve, mechanical threshold (E) and thermal sensitivity (F) in SNI-treated mice after ACC RARB overexpression (n = 10). (G, H) Contralateral stimulus-response curve, mechanical threshold (G) and thermal sensitivity (H) in SNI-treated mice after ACC RARB overexpression (n = 10). (I) Traveling trajectory in the EPM and quantitative summary of mice overexpressing RARB in open arm (n = 9-10). (J) TST summary in mice after overexpression of RARB in ACC (n = 8-11). (K) SPT in RARB-overexpressing Sham- and SNI-treated mice (n = 10). **P* < 0.05, ***P* < 0.01, ****P* < 0.001, *****P* < 0.0001. Statistical analysis was performed by 2-tailed unpaired *t* test (C, F, and H), Mann-Whitney *U* test (E and G), 1-way ANOVA (J and K) and Kruskal-Wallis *H* test (I). PWMT, paw withdrawal mechanical threshold; PWTL, paw withdrawal thermal latency.

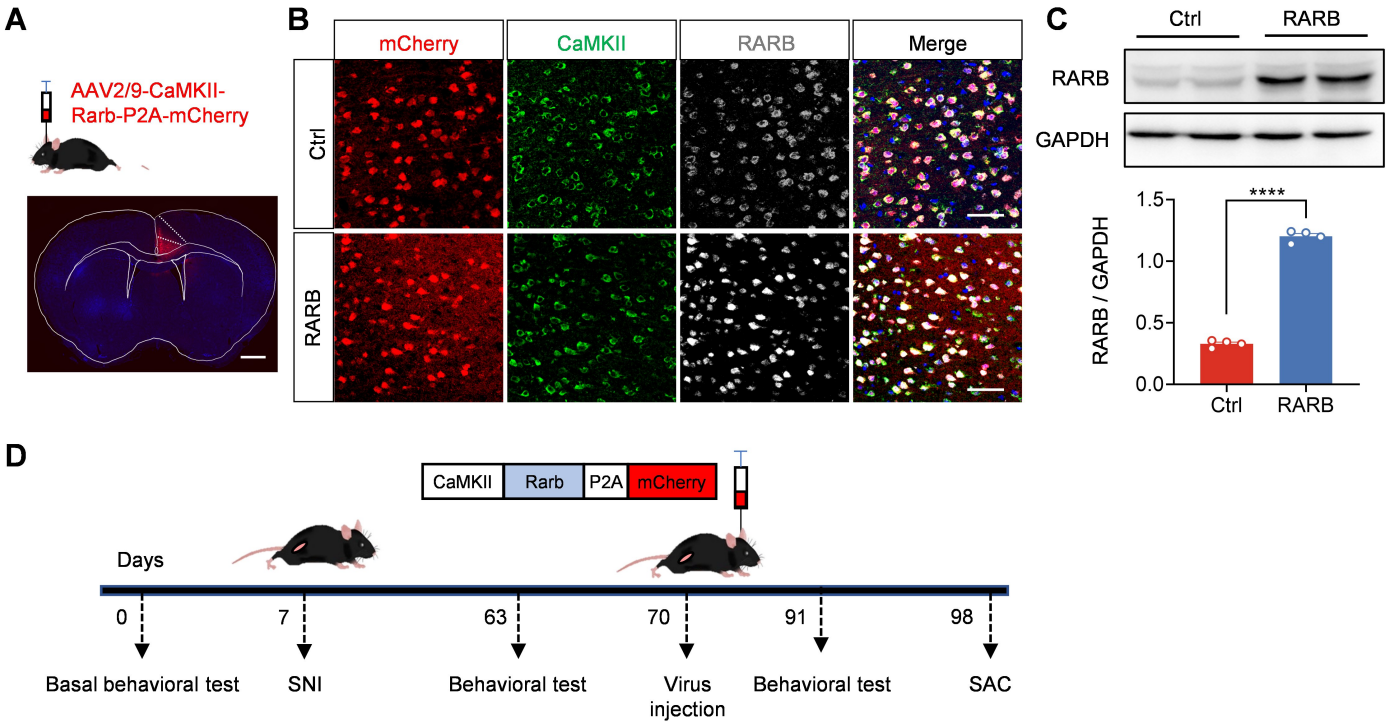
A
AAV2/9-CaMKII-
Rarb-P2A-mCherry
B
mCherry
CaMKII
RARB
Merge
Ctrl
RARB
C
Ctrl
RARB
RARB
GAPDH
RARB / GAPDH
****
Ctrl
RARB
D
CaMKII
Rarb
P2A
mCherry
Days
0
7
63
70
91
98
Basal behavioral test
SNI
Behavioral test
Virus
injection
Behavioral test
SAC

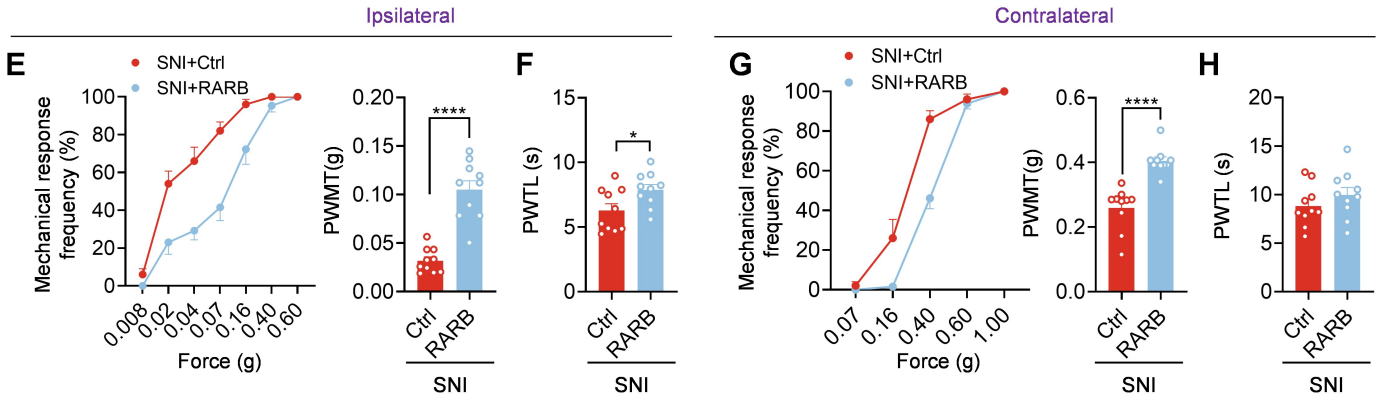
Ipsilateral
Contralateral
E
SNI+Ctrl
SNI+RARB
Mechanical response
frequency (%)
Force (g)
PWMT(g)
F
PWTL (s)
G
H
SNI

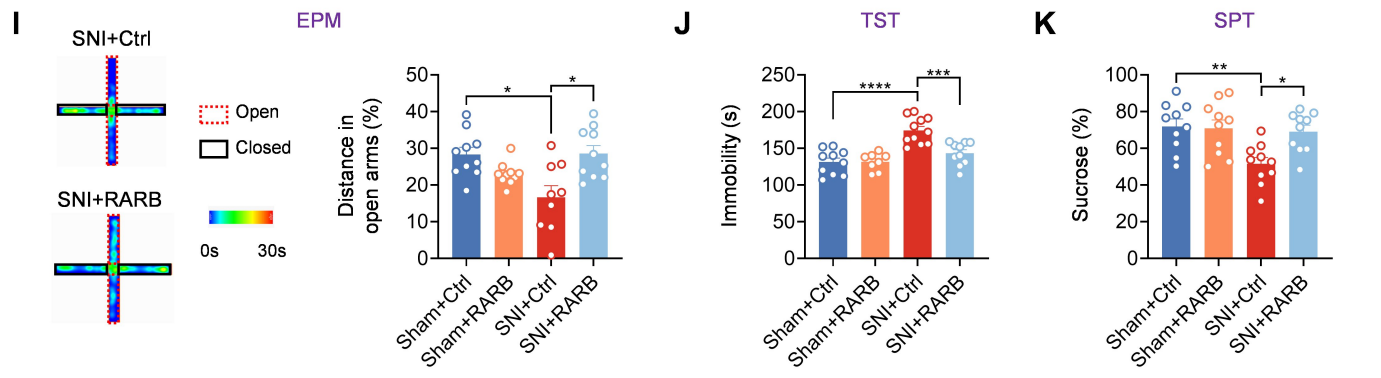
I
EPM
SNI+Ctrl
SNI+RARB
Open
Closed
0s
30s
Distance in
open arms (%)
J
TST
Immobility (s)
K
SPT
Sucrose (%)
Sham+Ctrl
Sham+RARB
SNI+Ctrl
SNI+RARB

Figure 3 RARB-overexpressing in ACC normalizes abnormal structural and functional plasticity induced by SNI. (A) Representative images of apical dendrites of ACC pyramidal neurons obtained from mice overexpressing RARB and control virus in both sham and SNI conditions. Scale bar: 5 μm. (B) Summary of spine density on the apical dendrites in the above four conditions (n = 17-20). (C) Summary of the density of stubby- and mushroom- shaped spines (n = 17-20). (D) Whole-cell patch-clamp recording from ACC layer II/III pyramidal neurons. Scale bar: 50 μm. (E) Action potentials (APs) in neurons after overexpressing RARB in both genotypes of mice. (F, G) I-O curve (F) and typical summary at intensity of 120 pA (G) after overexpressing RARB in sham- and SNI-treated mice (n = 8-11). (H) Rheobase after RARB overexpression in both types of mice (n = 8-11). (I, J) Representative traces (I) and I-O curve (J) of AMPAR-mediated eEPSCs after overexpressing RARB in SNI-treated mice (n = 8-10). (K, L) Typical examples (K) and quantitative summary (L) of PPR of eEPSCs after RARB overexpression in SNI condition (n = 10-12). (M, N) Representative traces (M), mEPSCs frequency and amplitude (N) after RARB overexpression in SNI-treated mice (n = 12). *P < 0.05, **P < 0.01, ***P < 0.001, ****P < 0.0001. Kruskal-Wallis H test (B and C), 2-way ANOVA (F and left panel in J), 1-way ANOVA (G and H), 2-tailed unpaired t test (L, and left panel in N) and Mann-Whitney U test (right panel in J, and right panel in N).

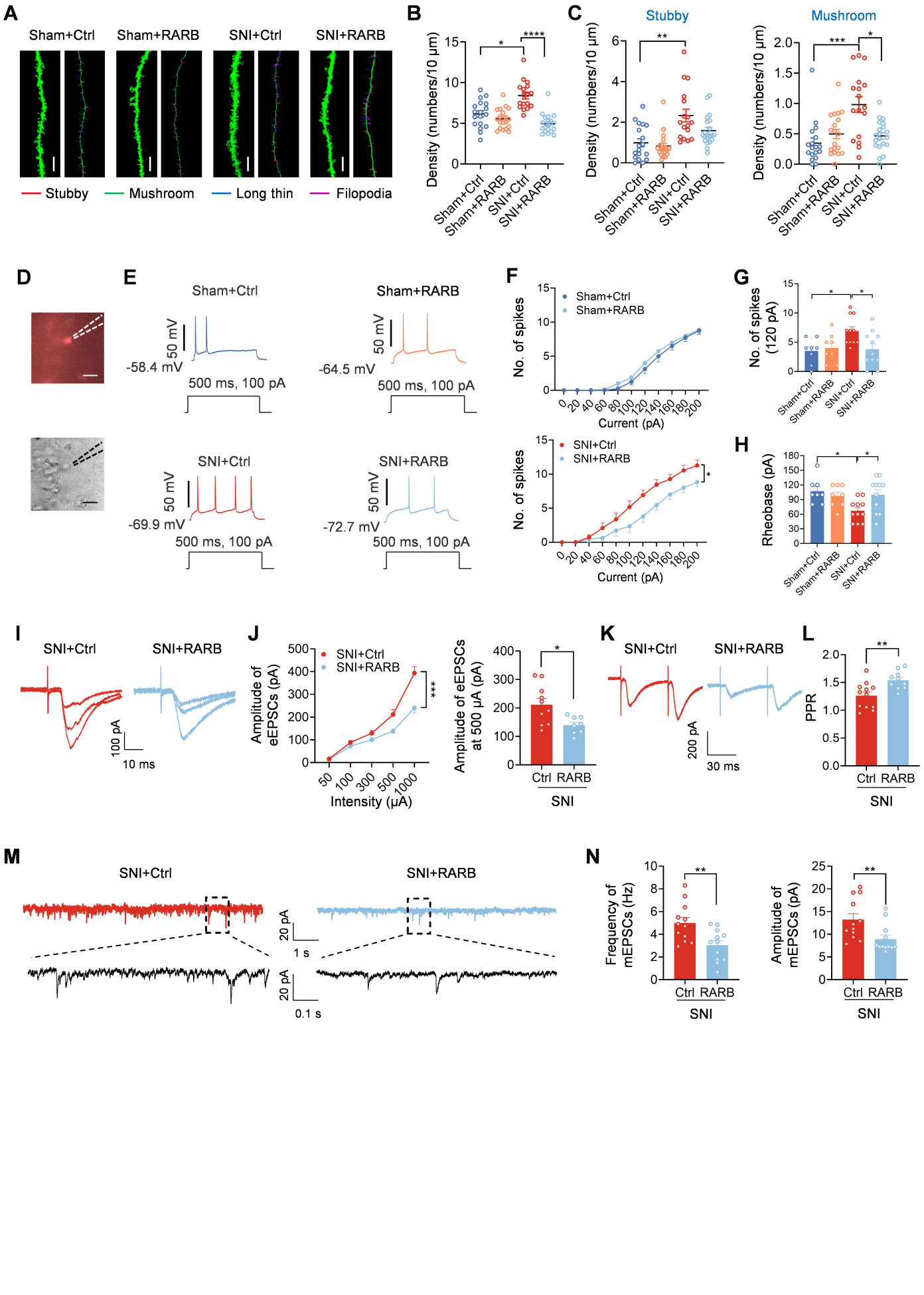
A
Sham+Ctrl
Sham+RARB
SNI+Ctrl
SNI+RARB
Stubby
Mushroom
Long thin
Filopodia
B
Density (numbers/10 μm)
C
Stubby
Mushroom
Density (numbers/10 μm)
D
E
Sham+Ctrl
Sham+RARB
SNI+Ctrl
SNI+RARB
50 mV
-58.4 mV
-64.5 mV
-69.9 mV
-72.7 mV
500 ms, 100 pA
F
No. of spikes
Sham+Ctrl
Sham+RARB
SNI+Ctrl
SNI+RARB
Current (pA)
G
No. of spikes (120 pA)
H
Rheobase (pA)
I
100 pA
10 ms
J
Amplitude of eEPSCs (pA)
Intensity (μA)
Amplitude of eEPSCs at 500 μA (pA)
Ctrl
RARB
SNI
K
200 pA
30 ms
L
PPR
M
20 pA
1 s
0.1 s
N
Frequency of mEPSCs (Hz)
Amplitude of mEPSCs (pA)

Figure 4 RARB-overexpressing in ACC alleviates neuronal hyperactivity induced by SNI. (A) Experimental schematic diagram showing virus injection, optical fiber implantation in ACC and fiber photometry recording during behavioral test in mice expressing control virus and RARβ. Scale bar: 1 mm (left) and 200 μm (right). (B-G) Representative photometry traces as shown in heat maps and quantitative summary from 5 independent experiments of peak GCaMP6s signals locked to the 0.4 g mechanical stimuli (B), 2 g mechanical stimuli (C), brush stimuli (D) and pinprick nociception (E) and radiant heat stimulation (F) and the onset of struggling during tail suspension (G). ***P < 0.001, ****P < 0.0001. B, C, E and F: Mann-Whitney U test, D and G: 2-tailed unpaired t test.

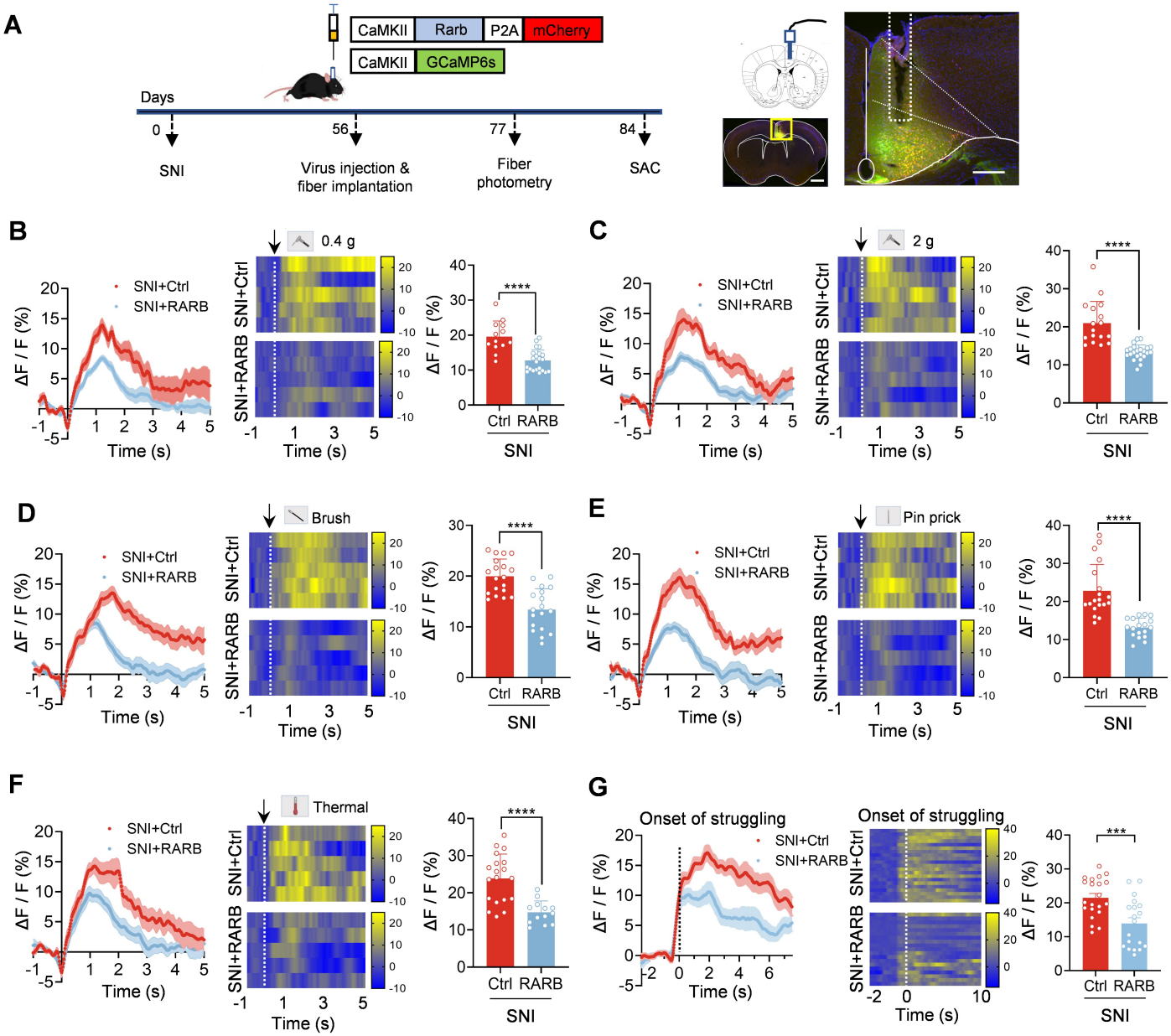
A
CaMKII
Rarb
P2A
mCherry
CaMKII
GCaMP6s
Days
0
56
77
84
SNI
Virus injection & fiber implantation
Fiber photometry
SAC
B
0.4 g
C
2 g
D
Brush
E
Pin prick
F
Thermal
G
Onset of struggling
SNI+Ctrl
SNI+RARB
ΔF / F (%)
Time (s)
Ctrl
RARB
SNI
****
***

Figure 5 RARB knockdown in ACC induces pain hypersensitivity and anxiodepression. (A) Schematic diagram showing intra-ACC virus injection. Scale bars: 1 mm (enlarged insets). (B, C) Double immunofluorescence (B) and western blotting (C) showing efficient RARB knockdown (n = 4). Scale bar: 30 μm in (B). (D) Schematic diagram showing virus injection in ACC and behavioral test in mice expressing scrambled shRNA and shRarb. (E and F) Ipsilateral stimulus-response curve, mechanical threshold (E) and thermal sensitivity (F) after ACC RARB knockdown in sham-treated mice (n = 12-16). (G) Traveling trajectory in the EPM and quantitative summary of sham-treated mice expressing shRarb in open arm (n = 11-13). (H) Traveling trajectory in the OFT and quantitative summary of sham-treated mice expressing shRarb in centre area (n = 11-13). (I) TST after expression of AAV-shRarb in sham-treated mice (n = 9-11). (J) SPT in shRarb-expressing Sham-treated mice (n = 10). (K-N) Representative photometry traces as shown in heat maps and quantitative summary from 5 independent experiments of peak GCaMP6s signals locked to von Frey hairs stimuli (0.4-2 g) (K, L), radiant heat stimuli (M) and the onset of struggling during tail suspension (N). *P < 0.05, **P < 0.01, ***P < 0.001, ****P < 0.0001. Statistical analysis was performed by Mann-Whitney U test (C, E, I, K and N) and 2-tailed unpaired t test (F-H, J, L and M).

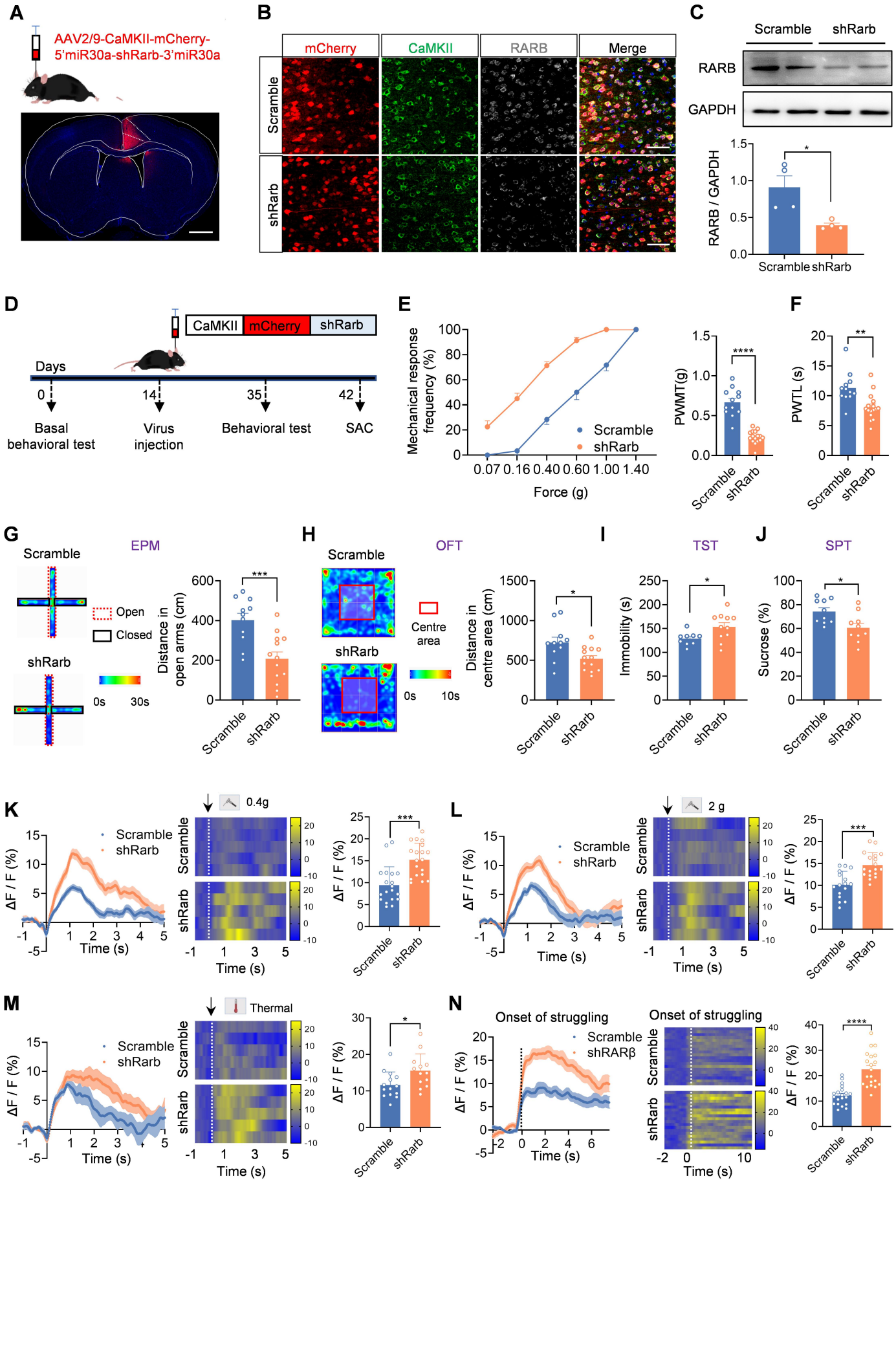
A
AAV2/9-CaMKII-mCherry-
5'miR30a-shRarb-3'miR30a
B
mCherry
CaMKII
RARB
Merge
Scramble
shRarb
C
Scramble
shRarb
RARB
GAPDH
RARB / GAPDH
Scramble shRarb
D
CaMKII
mCherry
shRarb
Days
0
14
35
42
Basal behavioral test
Virus injection
Behavioral test
SAC
E
Mechanical response frequency (%)
Force (g)
0.07 0.16 0.40 0.60 1.00 1.40
Scramble
shRarb
PWMT(g)
PWTL (s)
F
G
EPM
Open
Closed
0s
30s
Distance in open arms (cm)
H
OFT
Centre area
0s
10s
Distance in centre area (cm)
I
TST
Immobility (s)
J
SPT
Sucrose (%)
K
0.4g
ΔF / F (%)
Time (s)
L
2 g
M
Thermal
N
Onset of struggling
shRARβ

Figure 6 RARB regulates ECM remodeling via LAMB1 to modulate pain sensitivity and anxiodepression. (A, B) Representative immunoblots and quantitative summary of RARB and LAMB1 levels in ACC from mice expressing scrambled shRNA and shRarb (n = 4) (A) as well as control virus and RARB (n = 4) (B). (C) Luciferase activity after co-transfection of RARB-overexpressing plasmid and luciferase reporter plasmid connected with *Lamb1* promoter / *Lamb1* promoter mutant (n = 6-10). (D) Luciferase activity of vehicle and RA addition after co-transfection of RARB and *Lamb*1-Luc (n=7-8). (E) ChIP assay of levels of RARB binding with *Lamb1* promoter fragment in ACC from mice expressing Ctrl and RARB (n = 5). (F) A schematic model proposing RARB regulatory mechanism in the process of chronic pain. (G) Schematic diagram showing virus injection in ACC. (H and I) Stimulus-response curve and mechanical threshold (H) and thermal hyperalgesia (I) in SNI-treated mice followed by shLamb1 and/or overexpressing RARB treatment (n = 9-10). (J-L) OFT (J), EPM (K), and TST (L) in SNI-treated mice expressing shLamb1 and/or RARB (n = 8-10). (M, N) Representative SEM images (M) and fiber diameter (N) in control mice, SNI-treated mice, SNI-treated mice overexpressing RARB and sham-treated mice expressing shRarb (n = 3 mice per group). Scale bar: 5 μm (5K ×), 1.2 μm (20K ×), 500 nm (50K ×). **P* < 0.05, ***P* < 0.01, ****P* < 0.001, *****P* < 0.0001. Mann-Whitney *U* test (A for RARB). 2-tailed unpaired *t* test (A for LAMB1, B and D). Kruskal-Wallis *H* test (C, H, K, L and N) and 1-way ANOVA (E, I and J).

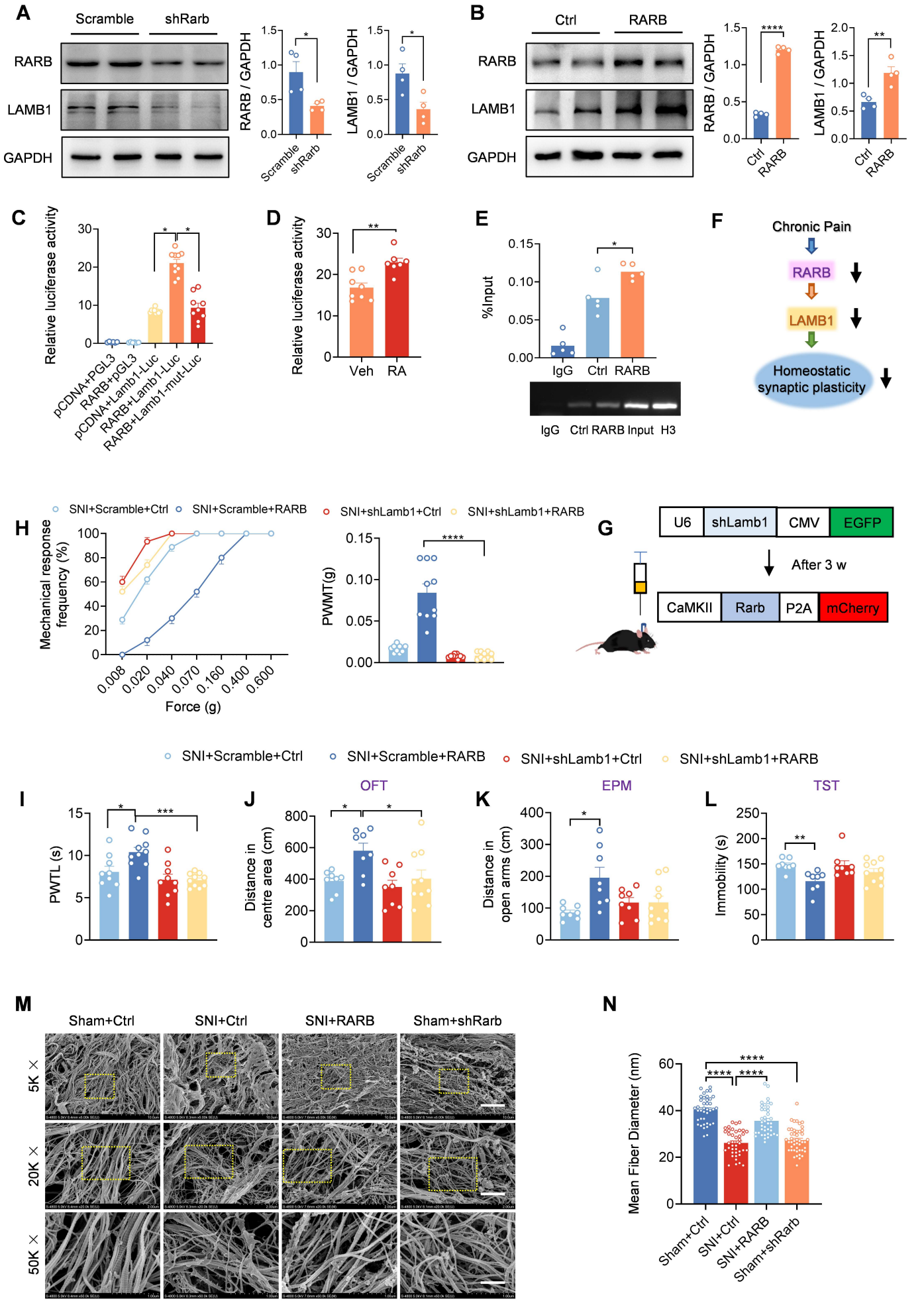
A
Scramble
shRarb
RARB
LAMB1
GAPDH
RARB / GAPDH
LAMB1 / GAPDH
B
Ctrl
RARB
C
Relative luciferase activity
pCDNA+PGL3
RARB+pGL3
pCDNA+Lamb1-Luc
RARB+Lamb1-Luc
RARB+Lamb1-mut-Luc
D
Veh
RA
E
%Input
IgG
Ctrl
RARB
IgG Ctrl RARB Input H3
F
Chronic Pain
RARB
LAMB1
Homeostatic synaptic plasticity
H
SNI+Scramble+Ctrl
SNI+Scramble+RARB
SNI+shLamb1+Ctrl
SNI+shLamb1+RARB
Mechanical response frequency (%)
Force (g)
PWMT(g)
G
U6
shLamb1
CMV
EGFP
After 3 w
CaMKII
Rarb
P2A
mCherry
I
PWTL (s)
J
OFT
Distance in centre area (cm)
K
EPM
Distance in open arms (cm)
L
TST
Immobility (s)
M
Sham+Ctrl
SNI+Ctrl
SNI+RARB
Sham+shRarb
5K ×
20K ×
50K ×
N
Mean Fiber Diameter (nm)

Figure 7 Retinoic acid levels are decreased in chronic pain comorbid with anxiodepression. (A) The table summarized the information of patients. The grouping are met the following conditions: *Healthy volunteers: NRS<3, GAD7≤4, HAMA≤6, HAMD≤8, PHQ9≤4; Chronic pain: NRS≥3, GAD7≤4, HAMA≤6, HAMD≤8, PHQ9≤4; Chronic pain comorbid with anxiety: NRS≥3, GAD7>4 and/or HAMA>6, HAMD≤8, PHQ9≤4; Chronic pain comorbid with depression: NRS≥3, GAD7≤4, HAMA≤6, HAM>8 and/or PHQ9>4; Chronic pain comorbid with anxiodepression: NRS≥3, GAD7>4 and/or HAMA>6, HAMD>8 and/or PHQ9>4; (B) ELISA assay of RA level in serum from patients (n = 2-22). (C, D) ELISA assay of RA level in serum (C) (n = 5-6) and ACC (D) (n = 4-8) after SNI surgery. (E) Schematic diagram showing construction of AAV2/9 expressing RARE-TK promoter-EGFP. (F) Fluorescence images of GFP expression in 293FT cells transfected with AAV-RARE plasmid after RA treatment. Scale bar: 20 μm. (G) Immunoblots and quantitative summary of GFP expression in 293FT cells transfected with AAV-RARE plasmid after RA (5 μM) treatment (n = 3). (H, I) Immunofluorescence (H) and quantitative summary (I) of GFP and RARB expression in ACC from SNI-treated mice expressing AAV-RARE (n = 4). Scale bar: 30 μm. (J) Luciferase activity of vehicle and RA addition in the transfection of *Rarb*-Luc (n = 6-12). *P < 0.05, **P < 0.01. Statistical analysis was performed by Kruskal-Wallis H test (B, D, and J), 1-way ANOVA (C), 2-tailed unpaired t test (G and I for RARB density) and Mann-Whitney U test (I for GFP density).

A

		Control*	Chronic Pain	Chronic pain comorbid anxiety	Chronic pain comorbid depression	Chronic pain comorbid anxiodepression
Age		23-55	19-56	28,33	23-68	17-71
Gender	Male	11	9	1	11	10
	Female	11	6	1	6	6
Number		22	15	2	17	16
Type of pain		None	musculoskeletal pain (12), neuralgia (3)	Musculoskeletal pain	Musculoskeletal pain (11), neuralgia (6)	Musculoskeletal pain (6), neuralgia (10)
Total		72				

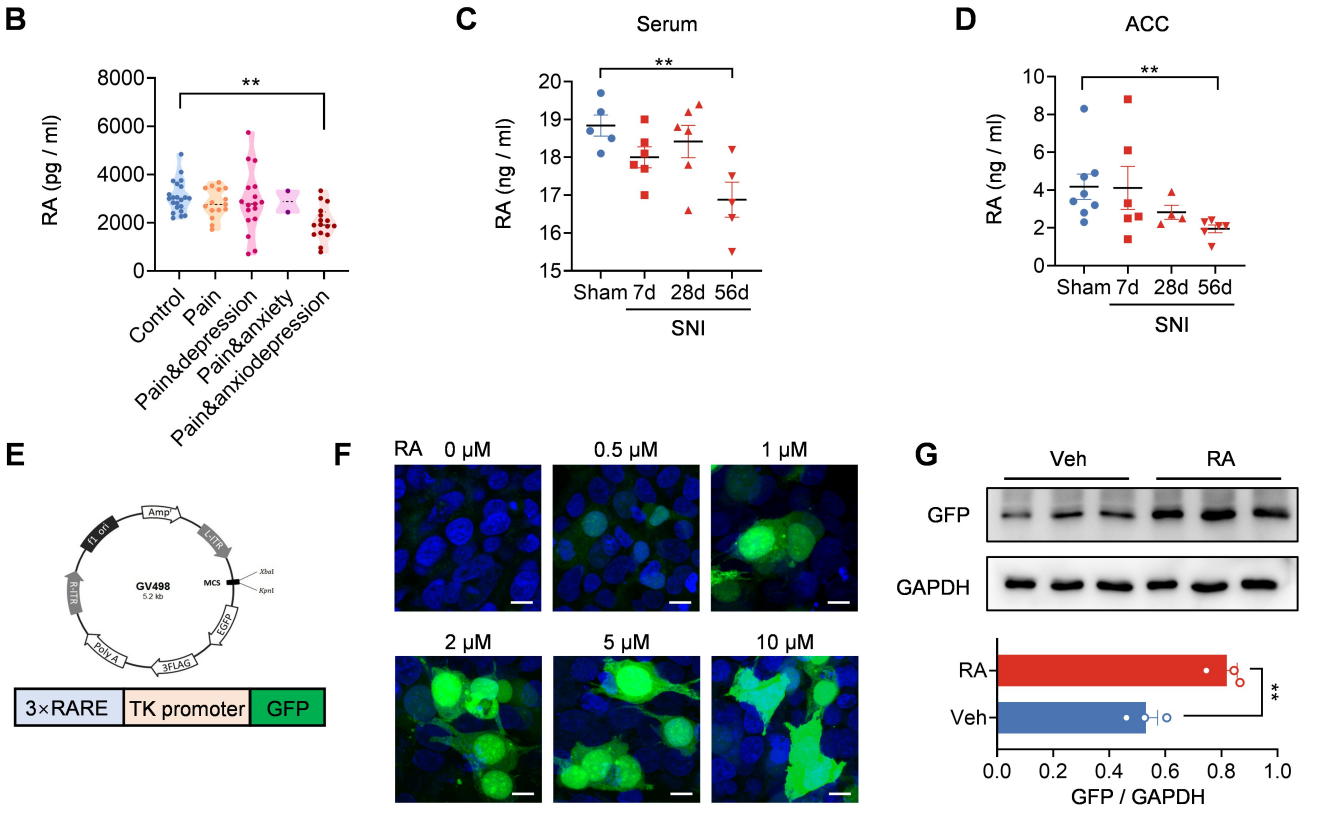

Figure 8 Administration of RA relieves established pain hypersensitivity and anxiodepression after SNI. (A) Schematic diagram of Intra-ACC injection of RA in SNI-treated mice. (B) Immunoblots and quantitative summary of LAMB1 and RARB protein level after ACC injection of RA. (C, D) Ipsilateral stimulus-response curves, mechanical threshold (C) and thermal latency (D) in SNI-treated mice followed by intra-ACC injection of RA (n = 10). (E) Open arm exploring in EPM test in SNI-operated mice after ACC delivery of RA (n = 7-10). (F) Centre area exploring in OFT test in SNI-operated mice after ACC delivery of RA (n = 7-10). (G, H) TST (G) and SPT (H) in SNI-operated mice after intra-ACC injection of RA (n = 7-15). (I) Schematic diagram of oral intake of RA (0.6 mg/Kg) in SNI-treated mice. (J, K) Ipsilateral stimulus-response curves, mechanical threshold (J) and thermal latency (K) in SNI-operated mice followed by oral intake of RA (n = 12). (L) Open arm exploring in EPM test in SNI-operated mice after oral RA (n = 12). (M) Centre area exploring in OFT test in SNI-operated mice after RA intake (n = 12). (N, O) TST (N) and SPT (O) in SNI-operated mice after RA intake (n = 9-12). *P < 0.05, **P < 0.01, ***P < 0.001, ****P < 0.0001. Statistical analysis was performed by 2-tailed unpaired *t* test (B, H, and K-O). Kruskal-Wallis *H* test (C and E), 1-way ANOVA (D, F, and G) and Mann-Whitney *U* test (J).

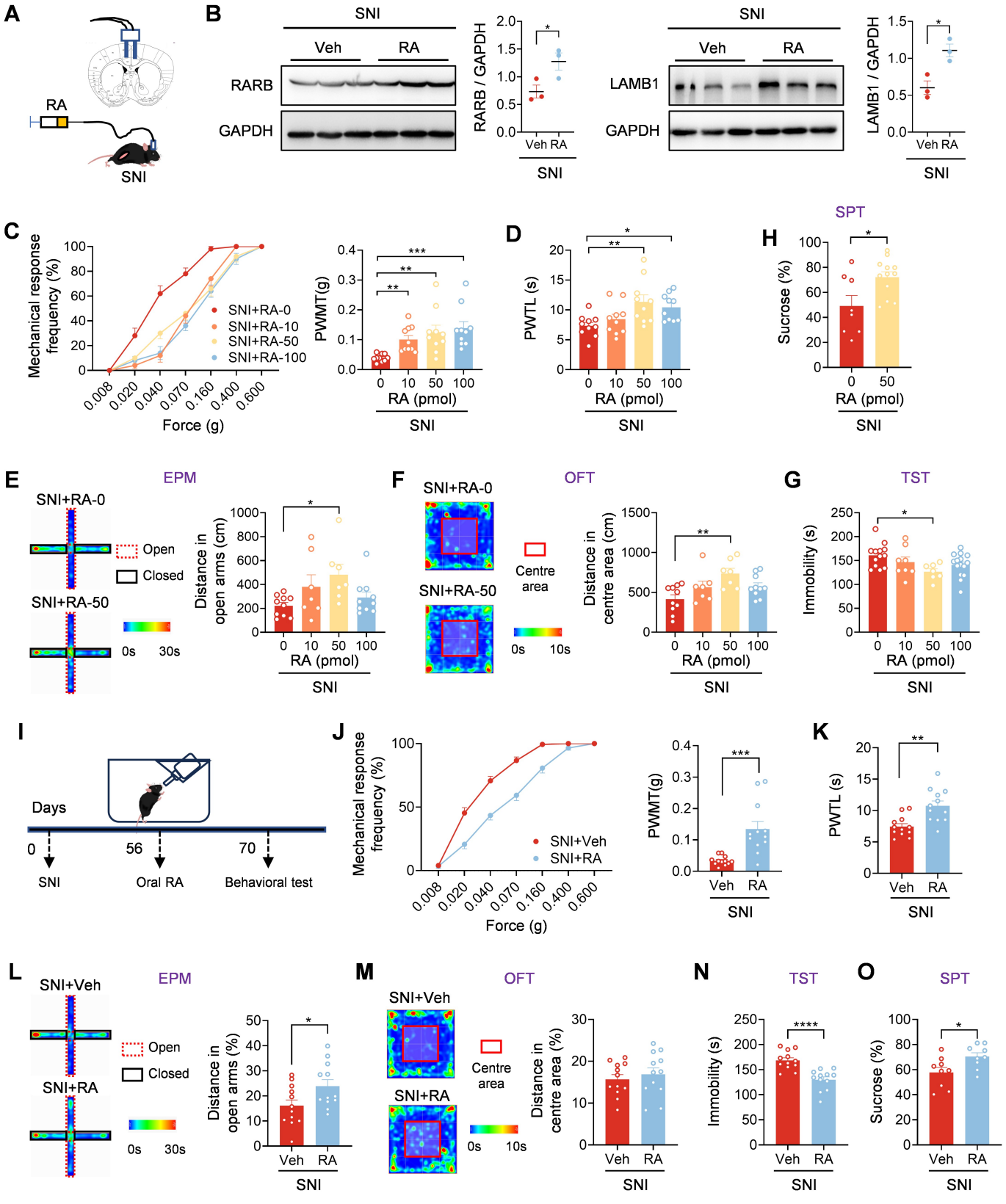
A
RA
SNI
B
SNI
Veh
RA
RARB
GAPDH
RARB / GAPDH
Veh RA
SNI
LAMB1
LAMB1 / GAPDH
C
Mechanical response frequency (%)
SNI+RA-0
SNI+RA-10
SNI+RA-50
SNI+RA-100
Force (g)
PWMT(g)
RA (pmol)
D
PWTL (s)
SPT
H
Sucrose (%)
E
EPM
SNI+RA-0
SNI+RA-50
Open
Closed
0s
30s
Distance in open arms (cm)
F
OFT
Centre area
Distance in centre area (cm)
G
TST
Immobility (s)
I
Days
0
56
70
Oral RA
Behavioral test
J
SNI+Veh
SNI+RA
K
L
M
N
O
Distance in open arms (%)
Distance in centre area (%)

Figure 9 RA alleviates neuronal overexcitation by regulating ECM microstructure through RARB after SNI. (A) Whole-cell patch-clamp recording from ACC layer II/III pyramidal neurons. Scale bar: 50 μm. (B, C) Action potentials (APs) at 100 pA (B) and I-O curve (C) after bath-applied RA (20 μM) (n = 10) (C). (D) Rheobase of neurons after delivery RA (n = 10). (E, F) Representative traces (E) and I-O curve (F) of AMPAR-mediated eEPSCs in SNI-treated mice prior to, during and washout of RA (n = 10-11). (G, H) Representative traces (G), time course and quantitative summary (H) of ACC LTP evoked by conditioning stimulus in the presence of RA (20 μM) and vehicle (n=7-8). (I, J) Confocal images (I) and quantitative summary (J) of GFP and RARB expression after delivery of TTX+AP5 in ACC from SNI-treated mice expressing AAV-RARE (n = 4). Scale bar: 200 μm (left) and 30 μm (right). (K, L) Representative SEM images (K) and quantitative summary (L) in SNI-treated mice with treatments at different magnification (n = 4 mice per group). Scale bar: 5 μm (5K ×), 1.2 μm (20K ×), 500 nm (50K ×). $^{**}P < 0.01$, $^{***}P < 0.001$, $^{****}P < 0.0001$. Statistical analysis was performed by 2-way ANOVA (left panels in C and F), 1-way ANOVA (right panel in C), Kruskal-Wallis *H* test (D, right panel in F, L) and 2-tailed unpaired *t* test (H, J).

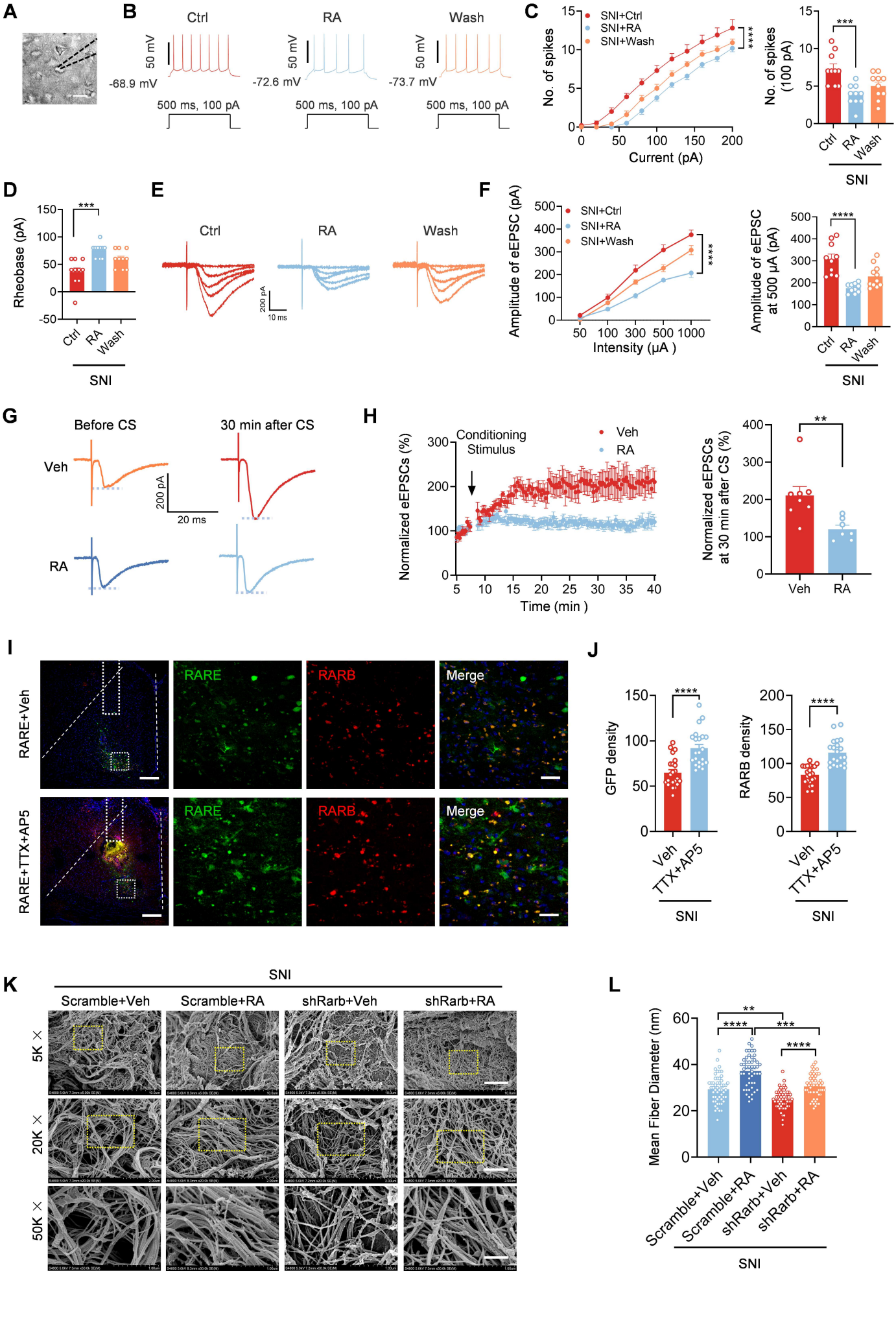
A
B
Ctrl
RA
Wash
50 mV
-68.9 mV
-72.6 mV
-73.7 mV
500 ms, 100 pA
C
SNI+Ctrl
SNI+RA
SNI+Wash
No. of spikes
Current (pA)
No. of spikes (100 pA)
SNI
D
Rheobase (pA)
E
200 pA
10 ms
F
Amplitude of eEPSC (pA)
Intensity (μA)
Amplitude of eEPSC at 500 μA (pA)
G
Before CS
30 min after CS
Veh
200 pA
20 ms
H
Conditioning Stimulus
Normalized eEPSCs (%)
Time (min)
Normalized eEPSCs at 30 min after CS (%)
I
RARE+Veh
RARE+TTX+AP5
RARE
RARB
Merge
J
GFP density
RARB density
Veh
TTX+AP5
K
Scramble+Veh
Scramble+RA
shRarb+Veh
shRarb+RA
5K ×
20K ×
50K ×
L
Mean Fiber Diameter (nm)

Figure 10 Administration of Talarozole relieves established pain hypersensitivity and anxiodepression after SNI. (A) Schematic diagram of Intra-ACC injection of TLZ in SNI-treated mice. (B, C) Ipsilateral stimulus-response curves, PWMT (B) and PWTL (C) in SNI-treated mice followed by intra-ACC injection of TLZ (n = 8-12). (D) Open arm exploring in EPM test in SNI-operated mice after ACC delivery of TLZ (n = 8-12). (E) Centre area exploring in OFT test in SNI-operated mice after ACC delivery of TLZ (n = 8-12). (F, G) TST (F) (n = 8-12) and SPT (G) (n = 5-6) in SNI-operated mice after intra-ACC injection of TLZ. (H) Schematic diagram of i.p. injection of TLZ in SNI-treated mice. (I, J) Ipsilateral stimulus-response curves, PWMT (I) and PWTL (J) in SNI-operated mice followed by administration of TLZ (n = 12). (K) Open arm exploring in EPM test in SNI-operated mice after injection of TLZ (n = 12). (L) Traveling trajectory in the OFT and quantitative summary after TLZ injection in SNI-operated mice (n = 12). (M, N) TST (M) and SPT (N) in SNI-operated mice after i.p. TLZ (n = 9-12). *P < 0.05, **P < 0.01, ***P < 0.001, ****P < 0.0001. Statistical analysis was performed by Kruskal-Wallis H test (B, F, I, L, M), 1-way ANOVA (C-E, G, J, K) and 2-tailed unpaired t test (N).

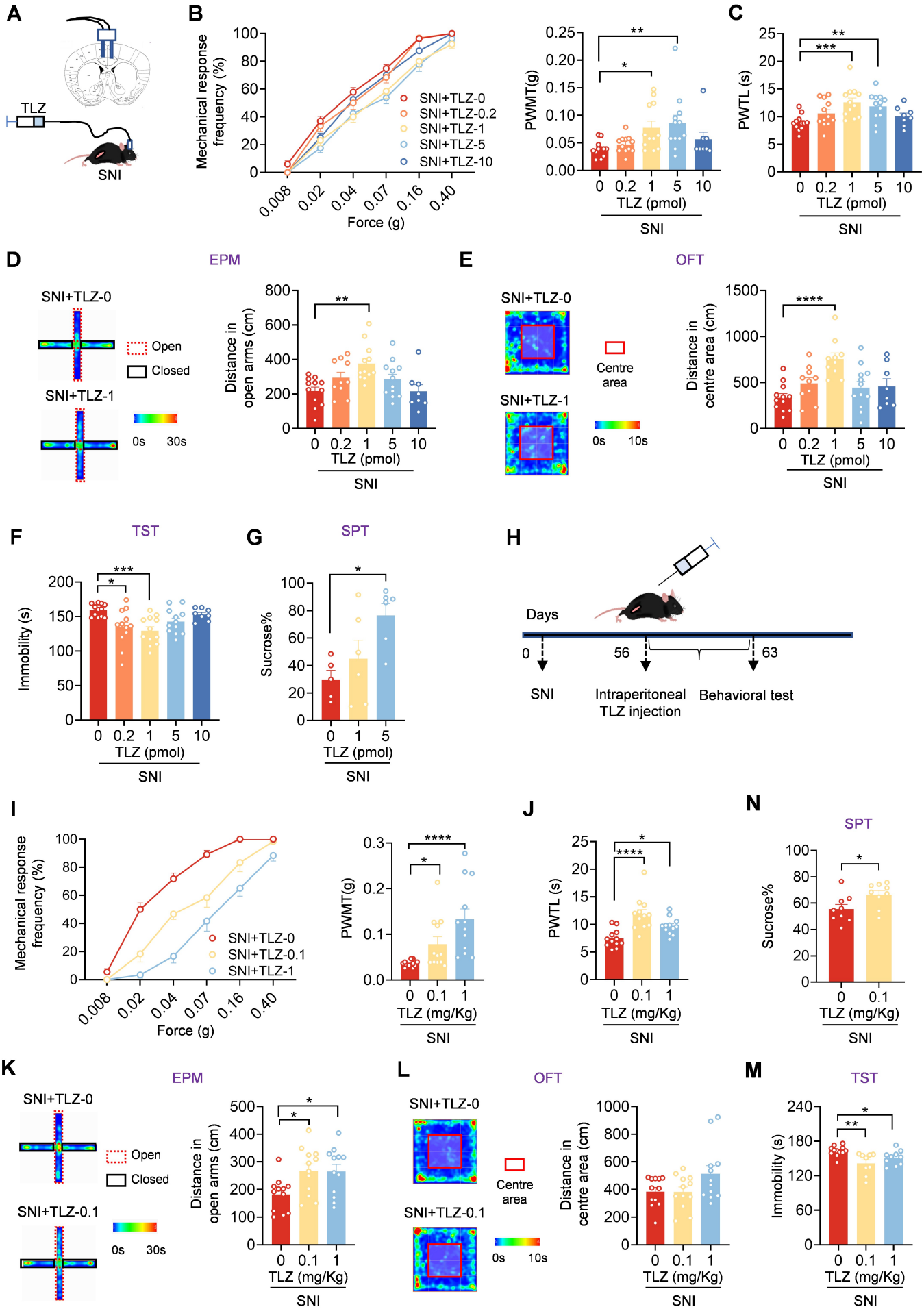
A
TLZ
SNI
B
Mechanical response frequency (%)
SNI+TLZ-0
SNI+TLZ-0.2
SNI+TLZ-1
SNI+TLZ-5
SNI+TLZ-10
Force (g)
PWMT(g)
TLZ (pmol)
SNI
C
PWTL (s)
TLZ (pmol)
SNI
D
EPM
SNI+TLZ-0
SNI+TLZ-1
Open
Closed
0s
30s
Distance in open arms (cm)
TLZ (pmol)
SNI
E
OFT
SNI+TLZ-0
SNI+TLZ-1
Centre area
0s
10s
Distance in centre area (cm)
TLZ (pmol)
SNI
F
TST
Immobility (s)
TLZ (pmol)
SNI
G
SPT
Sucrose%
TLZ (pmol)
SNI
H
Days
0
56
63
SNI
Intraperitoneal TLZ injection
Behavioral test
I
Mechanical response frequency (%)
SNI+TLZ-0
SNI+TLZ-0.1
SNI+TLZ-1
Force (g)
PWMT(g)
TLZ (mg/Kg)
SNI
J
PWTL (s)
TLZ (mg/Kg)
SNI
N
SPT
Sucrose%
TLZ (mg/Kg)
SNI
K
EPM
SNI+TLZ-0
SNI+TLZ-0.1
Open
Closed
0s
30s
Distance in open arms (cm)
TLZ (mg/Kg)
SNI
L
OFT
SNI+TLZ-0
SNI+TLZ-0.1
Centre area
0s
10s
Distance in centre area (cm)
TLZ (mg/Kg)
SNI
M
TST
Immobility (s)
TLZ (mg/Kg)
SNI

Figure 11 A schematic model proposing how cingulate RA/RARB homeostasis modulates neuropathic pain and associated anxiodepression via interaction with ECM LAMB1 through an intracellular-extracellular-intracellular feedforward regulatory network. See the text for details.

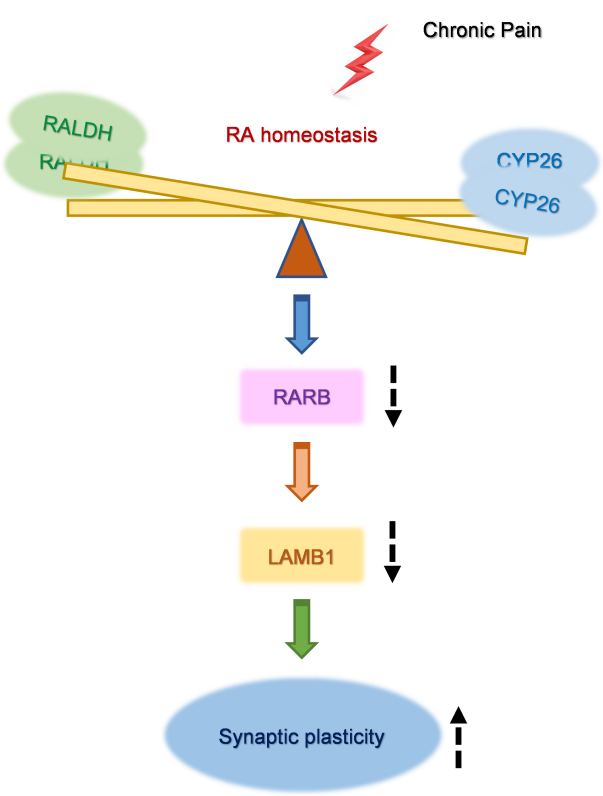
Chronic Pain
RALDH
RA homeostasis
CYP26
CYP26
RARB
LAMB1
Synaptic plasticity

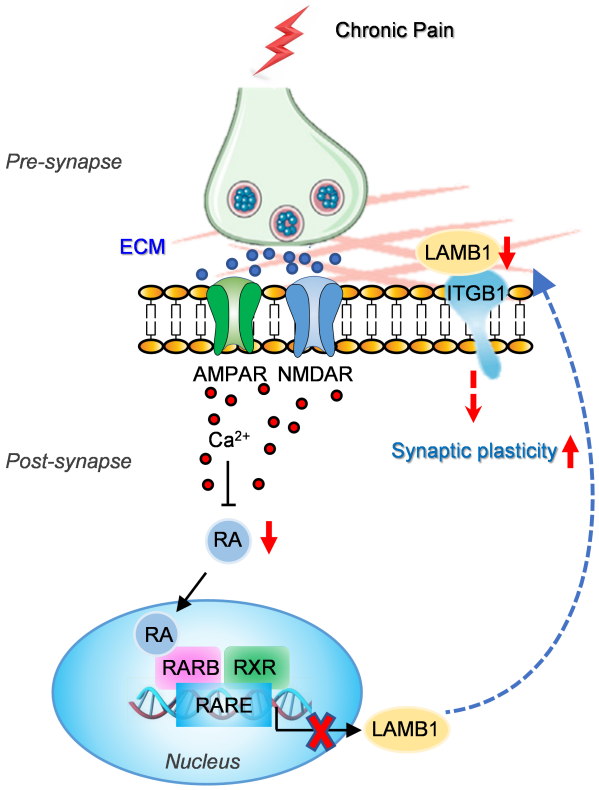
Chronic Pain
Pre-synapse
ECM
LAMB1
ITGB1
AMPAR
NMDAR
Ca2+
Post-synapse
Synaptic plasticity
RA
RA
RARB
RXR
RARE
LAMB1
Nucleus